



저작자표시-비영리-변경금지 2.0 대한민국

이용자는 아래의 조건을 따르는 경우에 한하여 자유롭게

- 이 저작물을 복제, 배포, 전송, 전시, 공연 및 방송할 수 있습니다.

다음과 같은 조건을 따라야 합니다:



저작자표시. 귀하는 원저작자를 표시하여야 합니다.



비영리. 귀하는 이 저작물을 영리 목적으로 이용할 수 없습니다.



변경금지. 귀하는 이 저작물을 개작, 변형 또는 가공할 수 없습니다.

- 귀하는, 이 저작물의 재이용이나 배포의 경우, 이 저작물에 적용된 이용허락조건을 명확하게 나타내어야 합니다.
- 저작권자로부터 별도의 허가를 받으면 이러한 조건들은 적용되지 않습니다.

저작권법에 따른 이용자의 권리는 위의 내용에 의하여 영향을 받지 않습니다.

이것은 [이용허락규약\(Legal Code\)](#)을 이해하기 쉽게 요약한 것입니다.

[Disclaimer](#)

Master of Science

**Polymerization of Hollow Core-Shell particle
Morphology and electrochemical performance**

The Graduate School of University of Ulsan

School of Chemical Engineering

Seung dong Seo

**Polymerization of Hollow Core-Shell particle
Morphology and electrochemical performance**

Supervisor: Professor Eun-suok Oh

A Dissertation

Submitted to
the Graduate School of the University of Ulsan
In partial Fulfillment of the Requirements
for the Degree of

Master

by

Seung dong Seo

School of Chemical Engineering

University of Ulsan, Korea

February 2019

Polymerization of Hollow Core-Shell particle
Morphology and electrochemical performance

This certifies that the master's thesis
of Seung Dong Seo is approved.

Committee Chair Prof. Eunwoo Shin

Committee Member Prof. Seunghyun Hur

Committee Member Prof. Jinsuk Chung

School of Chemical Engineering

University of Ulsan, Korea

February 2019

Acknowledgement

This research was supported by SAT Cooperation, Technopark of Ulsan and the Research of water-based polymer binder for super capacitor of electric vehicle project by ministry of SMEs and Startups. I would like to express sincere appreciation to them.

Furthermore, especially, I could have done this research thanks to all of my lab members who have taught and helped me to finish this work since I was just a beginner.

For the last, there is no way to express my appreciation enough to my professor, Eun-Suok Oh. Thank you for your passion and effort to be with your lab students, give knowledges, critically encourage us, always.

Thank you all the people being with and supporting me, always.

Abstract in Korean

최근 휴대용 전자기기의 발달과 함께 4차 산업혁명이 대두되면서 전지에 대한 연구는 더욱 더 중요시되고 있으며 현재는 자동차의 동력원이 될 만큼 대용량 및 고출력 특성을 지닌 전지가 개발되었다. 하지만 지금까지의 연구는 대부분 활물질에만 집중되어 왔으며 바인더에 대한 연구 비중은 비교적 작았다. 배터리의 안정성 및 성능 향상, 나아가서는 플렉서블 배터리의 실현을 위해서 바인더의 연구는 필수적이다. 본 연구에서는 코어-셀 고분자를 바인더로 활용하는 실험을 진행하였다. 코어-셀은 각 층에 사용되는 물질에 따라 다중특성을 지닐 수 있으며 물리적, 화학적 특성이 우수하여 염료, 약학 등 다양한 분야에 활용되고 있다. MMA-BA-MAA 공중합체 코어와 St-BA-AN 셀을 가진 코어-셀 고분자 입자를 중합하고 이를 알칼리제이션을 통해 코어물질을 제거 하여 할로우 코어-셀 고분자 입자를 중합하여 그 방법과 형태학을 분석하였다. 그리고 LTO 음극을 사용한 리튬이차전지 및 활성탄을 사용한 전기이중층커패시터 전극의 바인더로 활용해보았다. 이를 이용하여 전지를 제작하고 사이클 수명, 율속특성, 순환전압전류법, 임피던스 등 다양한 전기화학적 분석과 물리적 분석을 실시하였다.

Abstract in English

With the recent development of portable electronic devices and the advent of the fourth industrial revolution, the research of the battery has spurred further and it has now become a large-capacity and high-power energy storage system that can operate even the electric vehicle. Until these days, most of the researches on batteries have been focused on active materials, and research of binder has been relatively small. However, Binder research is essential to improve the stability and performance of batteries, and to realize flexible batteries.

In this research, the synthesis of core-shell and hollow core shell will be studied and the morphology of those polymers will be investigated. As a polymer binder in the electrode, the core shell and the hollow core-shell were applied in the electrochemical system such as LTO anode of lithium ion battery (LIB) and also activated carbon electrode of electric double layer capacitor (EDLC). First of all, in polymerization system, the MMA-BA-MAA copolymer emulsions were prepared as seed latices and the polymerization of MMA-MAA was consequently carried out to prepare core particles which have carboxyl group. The adhesive and conductive shell was then synthesized onto the core using St, BA, AN. The hollow polymer was obtained by alkalization treatment of the core-shell polymer using sodium hydroxide solution. With this polymers, LIB and EDLC were made and electrochemical performances were tested such as cycle, rate capability, CV, EIS.

Contents

Acknowledgement	I
Abstract in Korean	II
Abstract in English	III
Contents	IV
Figure list	VII
Table list	IX

1. Introduction

1.1. Definition of lithium ion battery	1
1.2. The components and principle of lithium ion batteries	1
1.3. Definition of electric double layer capacitor	3
1.4. The components and principle of electric double layer capacitor	3
1.5. The characteristics of electrode material	5
1.5.1. Lithium titanium oxide (LTO)	5
1.5.2. Activated carbon	5
1.6. Necessity of binder research : Hollow core-shell	5

2. Experimental

2.1. Hollow core-shell binder	8
2.1.1. Materials	8
2.1.2. Synthesis of hollow core shell binder	8

2.1.3. Alkalization treatment -----	8
2.2. Application to the LIB and EDLC -----	12
2.2.1. Preparation of LTO electrode of LIB -----	12
2.2.2. Preparation of activated carbon electrode of EDLC -----	12
2.2.3. Fabrication of 2032 coin cells of LIB and EDLC -----	12
2.3. Physical characteristics -----	16
2.3.1. Field emission - scanning electron microscopy (FE-SEM) -----	16
2.3.2. High resolution - Transmission electron microscopy (HR-TEM) -----	16
2.3.3 Fourier transform – infrared (FT-IR) -----	16
2.3.4. Differential scanning calorimetry (DSC) -----	16
2.3.5. Thermogravimetric analysis (TGA) -----	16
2.3.6. Particle size analysis (PSA) -----	17
2.3.7. Dispersion stability -----	17
2.3.8. Ionic conductivity -----	17
2.3.9. Adhesive force -----	17
2.3.10. Contact angle -----	18
2.3.11. Electrolyte uptake -----	18
2.4. Electrochemical characteristics -----	18
2.4.1. Galvanostatic charge/discharge test -----	18
2.4.2. Cyclic voltammetry (CV) -----	19
2.4.3. electrochemical impedance spectroscopy (EIS)-----	19

3. Results and discussion

3.1. Physical characteristics -----	20
3.1.1. FE-SEM and HR-TEM results -----	20

3.1.2. FT-IR results -----	20
3.1.3. DSC, TGA, PSA results -----	25
3.1.4. Dispersion stability results -----	29
3.1.5. Ionic conductivity results -----	33
3.1.6. Contact angle results -----	33
3.1.7. Adhesive force results -----	38
3.1.8. Electrolyte uptake results -----	40
3.2. Electrochemical characteristics -----	43
3.2.1. Cycle and rate capability results of LTO anode -----	43
3.2.2. CV results and calculation of diffusion coefficient of LTO anode -----	43
3.2.3. EIS results of LTO anode -----	48
3.2.4. Cycle and rate capability results of EDLC -----	50
3.2.5. CV results and calculation of diffusion coefficient of EDLC -----	50
3.2.6. EIS results of EDLC -----	53
4. Conclusion -----	55
5. Reference -----	56

Figure list

- Figure 1. Schematic illustration of charging/discharging process of LIB.
- Figure 2. Schematic illustration of charging/discharging process of EDLC.
- Figure 3. Schematic illustration of the effect of hollow core-shell binder on the electrode.
- Figure 4. Chemical structure of materials.
- Figure 5. Schematic illustration of alkalization of the core.
- Figure 6. Manufacturing process of the electrode of LIB.
- Figure 7. Schematic illustration of the electrode.
- Figure 8. 2032 coin cell assembly.
- Figure 9. HR-TEM results of Core (left) and Alkalized core (right)
- Figure 10. FE-SEM results of Core shell (left) and Hollow core shell (right)
- Figure 11. HR-TEM results of Core shell (left) and Hollow core shell (right)
- Figure 12. FT-IR results of Core, Alkalized core, Core shell and Hollow core shell
- Figure 13. DSC results of Core, Alkalized core, Core shell and Hollow core shell
- Figure 14. TGA results of Core, Alkalized core, Core shell and Hollow core shell
- Figure 15. PSA results of Core shell and Hollow core shell
- Figure 16. Turbiscan results of SBR 400B
- Figure 17. Turbiscan results of Core shell
- Figure 18. Turbiscan results of Hollow core shell
- Figure 19. Ionic conductivity results of SBR, Core, Alkalized core, Core shell, Hollow core shell
- Figure 20. Pictures of contact angle between each of binder films and LIB electrolyte
- Figure 21. Pictures of contact angle between each of binder films and EDLC electrolyte
- Figure 22. Adhesive force results of binder films of SBR, CS and HCS binders
- Figure 23. Pictures of binder films soaked in electrolytes for 144 hours
- Figure 24. Cycle and rate capability data of LTO cells comparing SBR, CS and HCS binders
- Figure 25. CV data of LTO cells comparing SBR, CS and HCS binders
- Figure 26. Computation of slope of peak currents vs. square root of voltage scan rate of LTO cells comparing SBR, CS and HCS binders from Randle-sevcik equation
- Figure 27. EIS data of LTO cells comparing SBR, CS and HCS binders
- Figure 28. Cycle and rate capability data of EDLC comparing SBR, CS and HCS binders
- Figure 29. CV data of EDLC comparing SBR, CS and HCS binders

Figure 30. EIS data of EDLC comparing SBR, CS and HCS binders

Table list

Table 1. Recipe for the hollow core shell polymer

Table 2. Contact angle results of SBR, CS and HCS with LIB and EDLC electrolytes

Table 3. Weights (mg) of binder films at the beginning and fully dried after 144 hours

Table 4. Diffusion coefficient of LTO cells of both of SBR, CS and HCS samples

Table 5. Diffusion coefficient of EDLC of both of SBR and HCS samples

1. Introduction

1.1. Definition of lithium ion battery

The battery can be called energy storage system(ESS). From various energy sources such as the sun, water, wind, fuels, energy can be generated in many forms such as heat, kinetic, electric energy. The battery stores energy changing electric energy to chemical energy. There are two types of battery. One is the primary battery which means it is not rechargeable such as mercury dry battery. The other one is the secondary battery which means rechargeable especially, for example as we all know well, lithium secondary battery(LIB). It has appeared in the world by Sony in Japan for the first time. LIB generates the energy from redox reaction at the cathode and anode, moving of Li^+ cation in the electrolyte, which means moving of charge. [1]

1.2. The components and principle of lithium ion batteries

The LIB consists largely of cathode, anode, separator and electrolyte. Lithium metal oxide is usually used as cathode active material such as lithium cobalt oxide and lithium manganese oxide and etc. And graphite, LTO are typical anode materials. when the battery is charged by external force, voltage, Li^+ cation separates from the cathode and pass through the electrolyte and separator finally get to the anode, then is combined with anode active material, which means storage of chemical energy. Otherwise when the battery is discharged, Spontaneously Li^+ cation separates from the anode and get to the cathode which means operating of electric energy. For the separator, polyethylene or polypropylene are usually used. For the electrolyte LiPF_6 dissolved in organic solvent such as ethylene carbonate, ethyl methyl carbonate is usually used. And conductive materials, binders and other additives should be added when electrode slurry is made. [1-3]

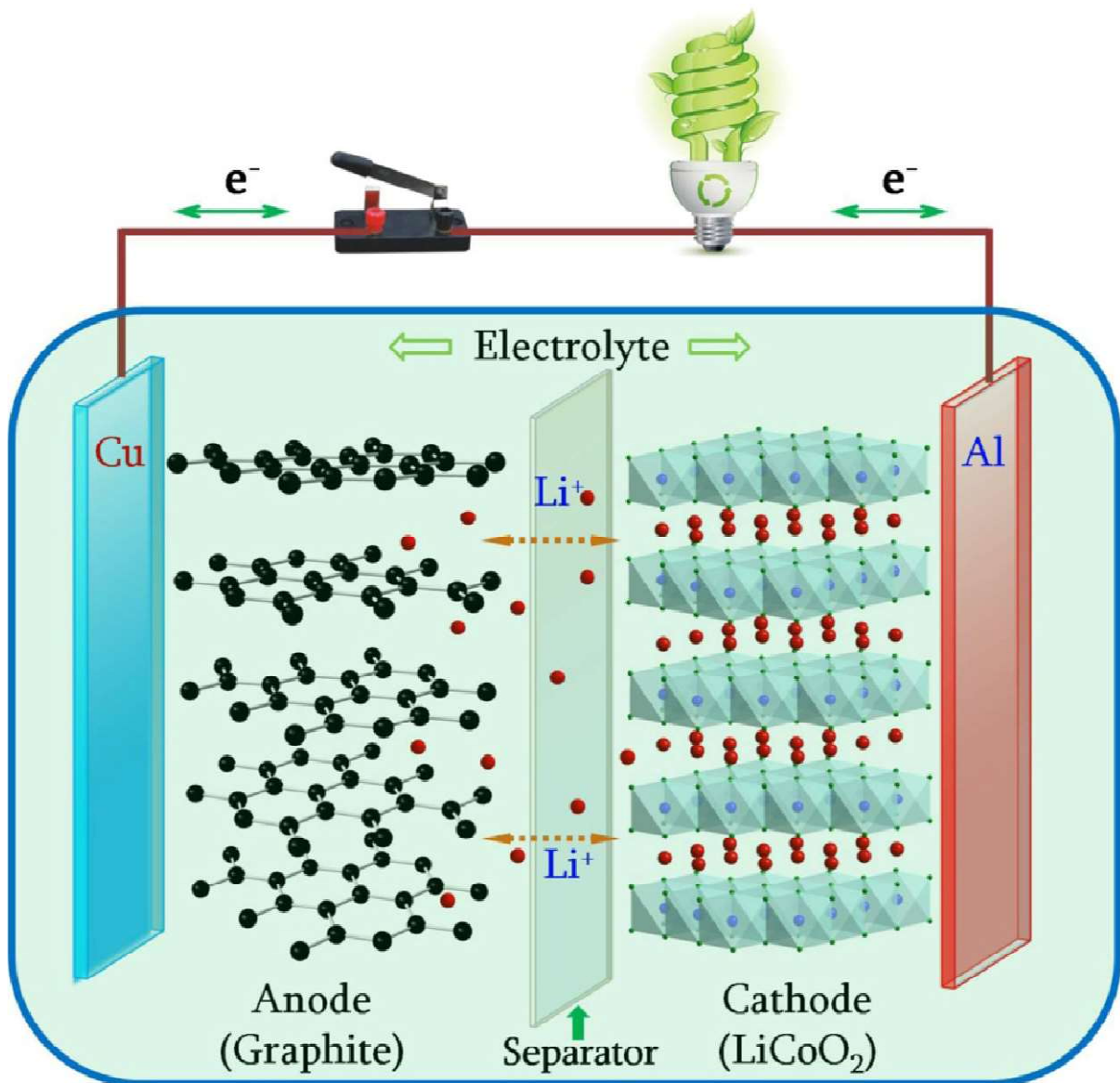


Figure 1. Schematic illustration of charging/discharging process of LIB [4]

1.3. Definition of electric double layer capacitor

Capacitor is also a kind of ESS which stores energy. But unlike the LIB, cathode and anode are not defined in the capacitor system because both of electrode have same coatings of slurry that include activated carbon as a active material. And there is no chemical reaction in the system. Due to this property, capacitor has a much higher output of power than LIB but also lower capacity than LIB. And also there is no operating voltage with the reason of no redox reaction. So in the voltage range, current is not that different as voltage change. To improve the capacity, electric double layer capacitor(EDLC) has been investigated. By using electrolyte which has large amount of ions and high ionic conductivity, electric double layer is made on the surface of electrode. It can cancel out the charge of electrode so that more electrons can move and be stored. Furthermore, electric double layer itself can store the energy by arranging ions. [5-6]

1.4. The components and principle of electric double layer capacitor

The active material of capacitor is commonly activated carbon that has huge surface area. when the capacitor is charged by external voltage, electrons move from one electrode that would be positive to the other electrode that would be negative. Then because of charge difference of both side of electrode, the energy stored. But with electrolyte of ions, cations diffuse to the negative electrode and anions diffuse to the positive electrode. As a result, charged ions cancel out the charge of each electrode surface, finally, more electrons can move and energy can be stored more than normal capacitor. [5-6]

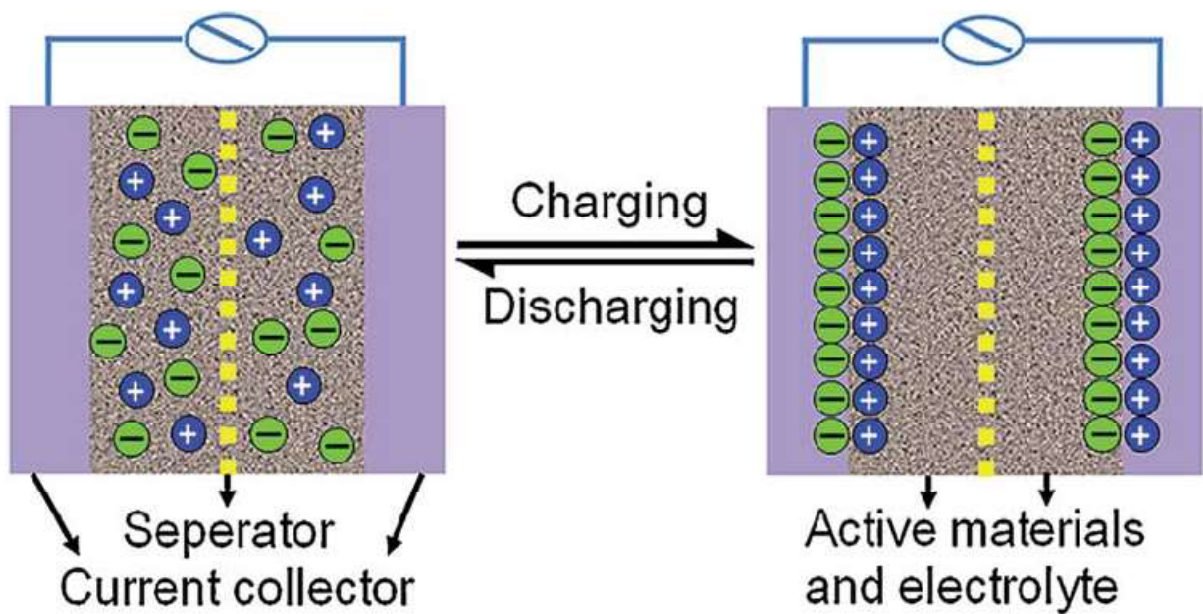
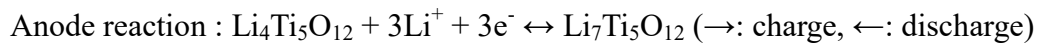


Figure 2. Schematic illustration of charging/discharging process of EDLC [6]

1.5. The characteristics of electrode materials

1.5.1. Lithium Titanium oxide (LTO)

LTO is spotlighted as an active material of anode nowadays because of its high operating voltage, low volume expansion and the characteristic of high output of power. when the energy is stored, Li^+ cation from cathode comes to the anode getting electron, react with LTO. This reaction happens at around 1.55 V (vs. Li^+/Li) that is quite high. Therefore, solid electrolyte interphase (SEI) layer doesn't appear in LTO cells [7]. Also the possibility of side reactions of other materials except active materials is relatively low enough. Theoretically, it has 175mAh/g energy density and normally volume expansion is negligible [8].



1.5.2. Activated carbon

Activated carbon has lots of macro, meso, micro pores. because of pores, surface of activated carbon is extremely huge, larger than $1000 \text{ m}^2/\text{g}$ [5]. So large amount of charge can be held on the surface. Activated carbon itself doesn't have any reaction in a common voltage range. It is operated normally in $0.1 \text{ V} \sim 2.7 \text{ V}$.

1.6. Necessity of binder research : Hollow core shell

The binder is one of the most important content of electrode for stability, high performance, furthermore, flexibility. The binder should endure the range of operating voltage of the battery. The highest occupied molecular orbital and the lowest unoccupied molecular orbital between the binder and the electrolyte should be investigated. Nowadays also along with the flexible display, flexible battery is being researched a lot. Finally, for the high performance, conductive materials such as carbon nano tube, graphene are utilized as the binder. Also, to make the coatings on the electrode stable against the strain from the fast electrochemical reaction which means high output of power, high adhesive force is necessary.

However, the core-shell polymer is receiving attention from all over the world nowadays. Because it can have various properties depending on what material it is made of, it has enormous probability to be used in many fields. For example, unlike homogeneous particles, core and shell have largely different refractive indexes of light. As a result, the scattering of the light occurs, and

the opacity and shielding property of the coating greatly increase. Therefore, polymer particles are utilized as an opacifying agent or a white pigment. And also it can be used as a medicine. To make the drug affect targeting spot, stable shell materials against pH or enzyme is polymerized on the affective curing core materials so that it can pass through the extreme conditions such as stomach [9-10]. In this research, morphology and application to the electrochemical system of core-shell and hollow core-shell polymer were mainly investigated. This might be useful as a binder which could help to improve both of mechanical and chemical properties of the electrode and its electrochemical performances. First, because the inside of the particle is empty, the particle can easily transform its shape like a air less ball. As a result, flexibility can be improved. Second, with the same reason, ions in the electrolyte can pass freely through the shell. In other words, interface area between active materials and electrolyte would be increased. Finally, it leads to the higher output of power. Third, after hollow process, ions from decomposition of core increase the viscosity of binder solution. So we may do not have to use CMC anymore [11].

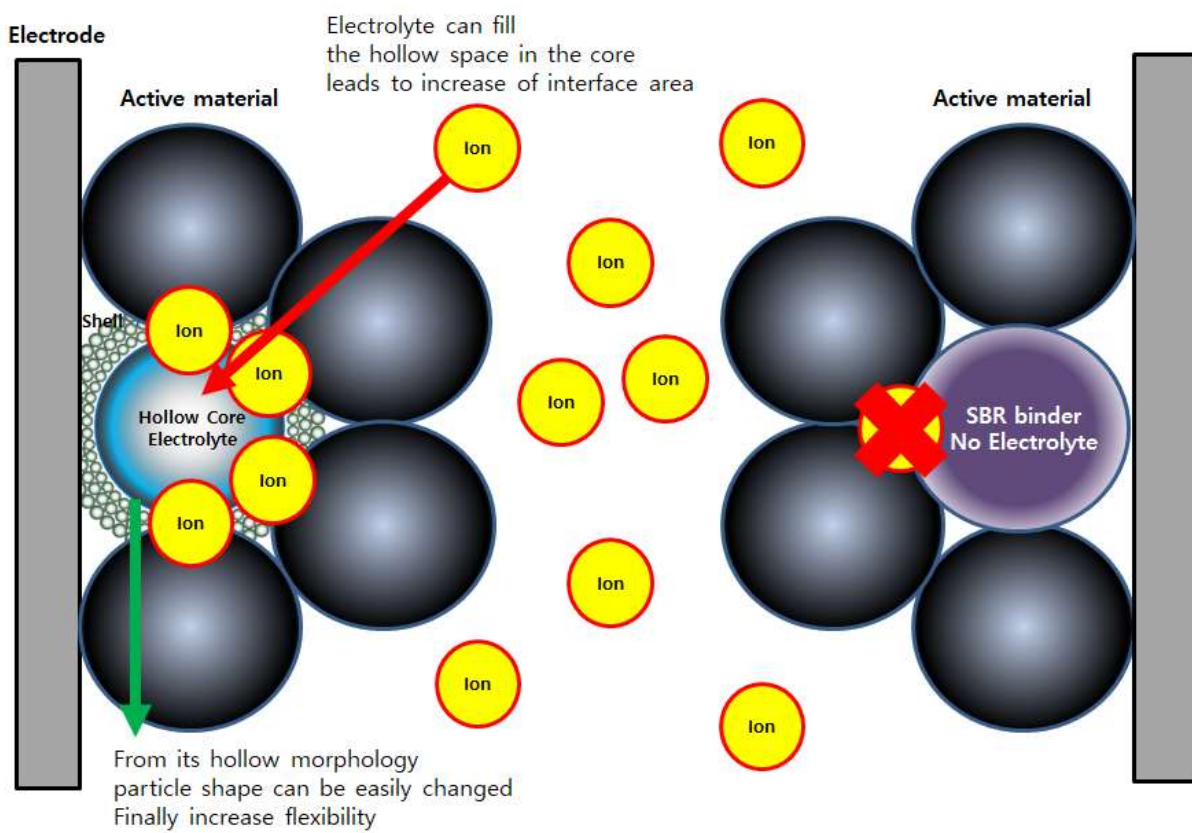


Figure 3. Schematic illustration of the effect of the hollow core-shell binder on the electrode

2. Experimental

2.1. Hollow core shell binder

2.1.1. Materials

Styrene (St, SAMCHUN), methyl methacrylate (MMA, Sigma aldrich), methacrylic acid (MAA, Sigma aldrich), butyl acrylate (BA, SAMCHUN) and acrylonitrile (AN, JUNSEI) were used as monomers. Divinylbenzene (DVB, Sigma aldrich) was used as crosslinking comonomer. Ammonium persulfate (APS, Sigma aldrich) and sodium dodecylbenzene sulfonate (SDBS, Sigma aldrich) were used as initiator and surfactant. Sodium hydroxide was used for alkalization treatment.

2.1.2. Synthesis of core-shell binder

The emulsion polymerization was conducted in a four-neck double jacket flask reactor equipped with a mechanical stirrer, reflux condenser, feeding pump and nitrogen gas purging system. The expected core-shell latex particles were prepared according to the recipe in Table 1. First, in the seed stage, emulsion was prepared by mixing distilled water, monomers and all of other additives were continuously fed into the reactor for 2 h at target temperature. Also, in the core stage, same feeding way was conducted for 2 h. Finally, in the shell stage, monomers and crosslinking agent and other additives with distilled water were separately fed into the reactor for 3 h. At all of steps, nitrogen purge was conducted and stirring speed was 200 rpm.

2.1.3. Alkalization treatment

To remove the core by decomposition of MMA-BA-MAA copolymer, alkalization treatment was conducted following Table. 1. Core-shell latex was mixed with 15 wt% solution and stirred by heating-magnetic stirrer in speed of 1000 rpm at 90°C. MMA-BA-MAA copolymer was ionized by neutralization reaction and became ionized carboxyl salt MMA-BA-R-COO⁻. As ionized core polymer got dissolved in the water, viscosity increased a lot. Therefore, addition of surfactant and water is needed.

Components	Seed latex (g)	Core latex (g)	Shell latex (g)	Alkalization treatment (g)
MMA	5.5	23	—	—
MAA	0.56	10	—	—
BA	6.5	—	40	—
St	—	—	40	—
AN	—	—	20	—
DVB	—	—	1	—
APS	1.0	0.562	0.8	—
SDBS	0.06	0.099	0.2	0.1
Seed latex	—	50	—	—
Core latex	—	—	130	—
Shell latex	—	—	—	30
Distilled water	500.0	250	55	20
15 wt% NaOH sol.	—	—	—	5
Temperature/°C	80	80	75	90

Table 1. Recipe of the hollow core shell polymer.

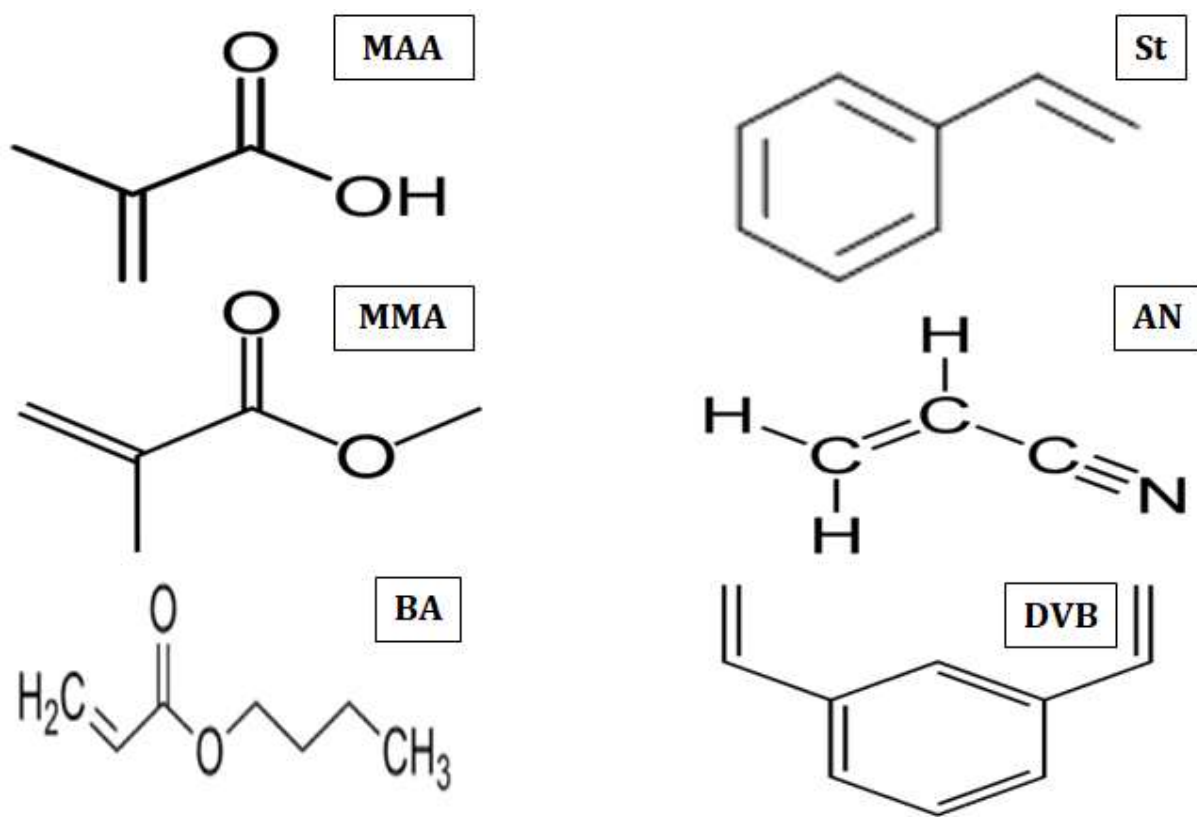


Figure 4. Chemical structures of materials.

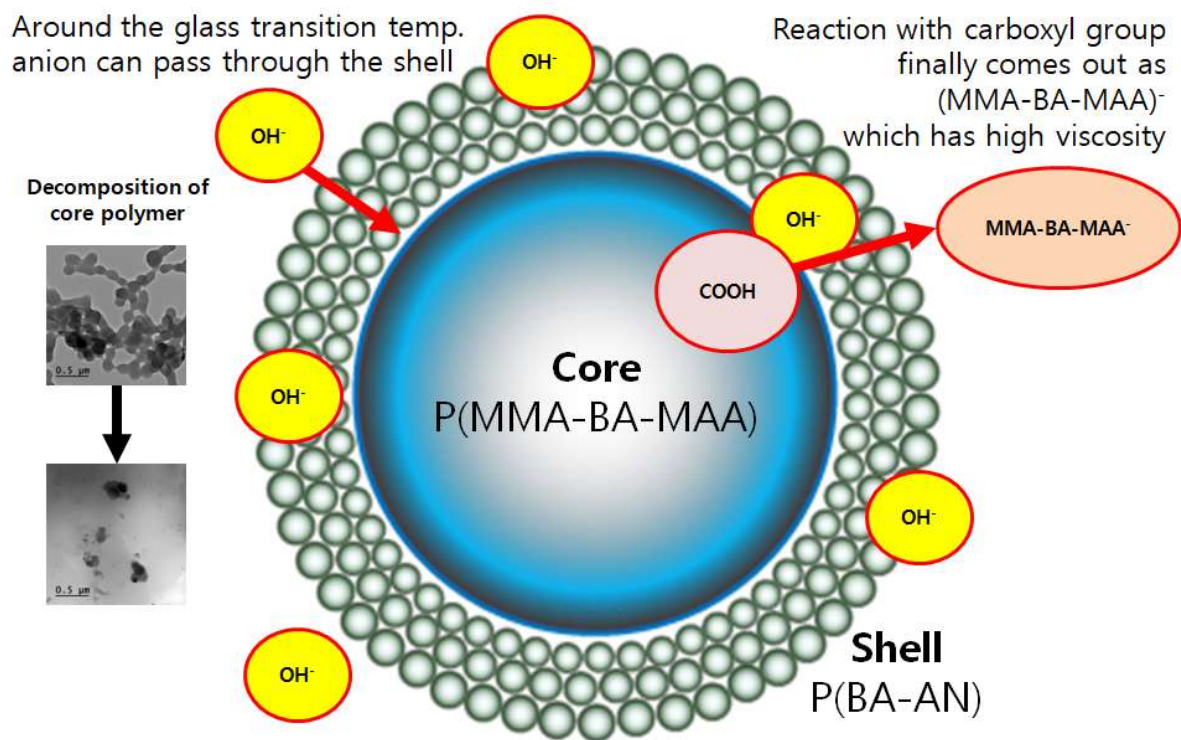


Figure 5. Schematic illustration of the alkalization of the core.

2.2. Application to the LIB and EDLC

2.2.1. Preparation of LTO electrode of LIB

Lithium titanium oxide (LTO, $\text{Li}_4\text{Ti}_5\text{O}_{12}$, Posco ESM) for the active material, carbon black (Super-P, Phoenix materials) for the conductive material, Carboxymethyl cellulose (CMC, Sigma aldrich) and distilled water for controlling viscosity were mixed with balls by planetary ball mill mixer (PULVERISETTE 7, FRITSCH). After mixing, for the final step, the binder sample was added and mixed. The final slurry was coated on the copper foil which thickness is $18\mu\text{m}$ with 10 mm/s of coating speed and dried in a convection oven at 60°C . Electrodes were slit in width of 2 cm and pressed by roll press machine.

2.2.2. Preparation of activated carbon electrode of EDLC

Activated carbon (YP-50, Kuraray) for the active material, Super-P for the conductive material, CMC (WS-C, Dai-ichi Kogyo Seiyaku Co.) and distilled water for controlling viscosity were mixed with balls by planetary centrifugal mixer (ARE-310, THINKY). Then the binder sample was added and mixed at the final. The slurry was coated on the etched aluminum foil with 10 mm/s of coating speed and dried in the convection oven at 60°C . Electrode was slit in width of 2 cm and pressed by roll press machine.

2.2.3. Fabrication of 2032 coin cells of LIB and EDLC

Components of 2032 coin cell are case, gasket, spacer disk, spring and cap. First, the electrode was located on the case, coated face should be up. Second, electrolyte which has components of, for LIB, 1M LiPF_6 in EC:EMC:DMC=1:1:1 by volume from Soulbrain, for EDLC, 1M tetraethylammonium-tetra-fluoroborate (TEABF_4) in acetonitrile was injected. the separator (Polypropylene, Welcos) was put on the electrode and then gasket was put. Third, in case of LIB, lithium metal was located, otherwise, in case of EDLC, same electrode facing to each electrode. Finally, spacer disk, spring and cap were assembled to connect all of components in the cell with stability.

- ① Active material
- ② Conductive material
- ③ binder and water

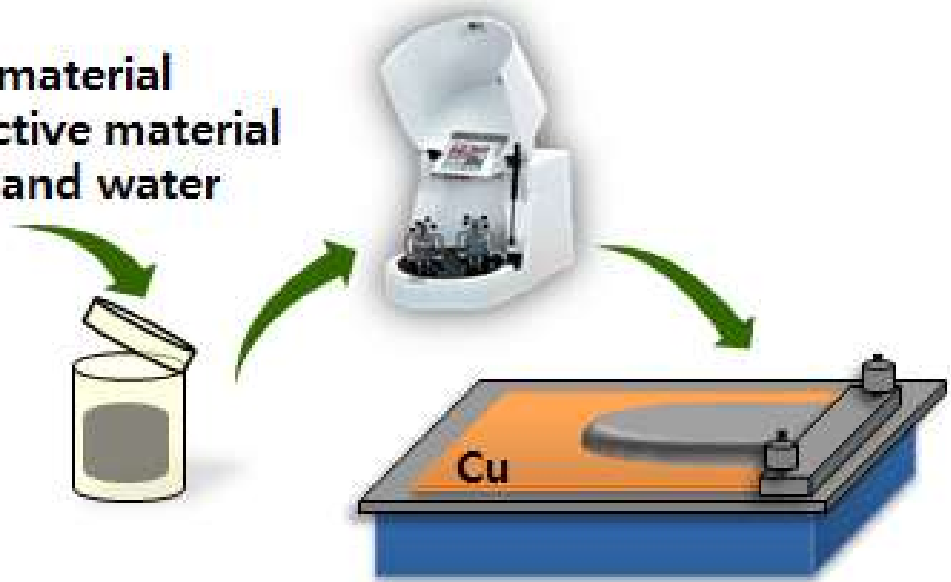


Figure 6. Manufacturing process of the electrode of LIB

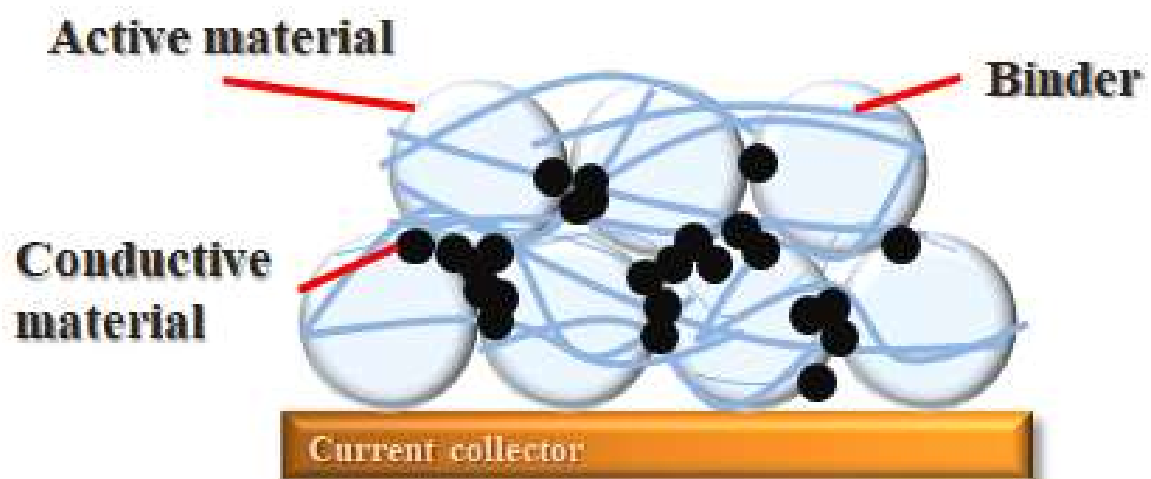


Figure 7. Schematic illustration of the electrode



Figure 8.2032coin cell assembly [13]

2.3. Physical characteristics

2.3.1. Field emission - Scanning electron microscopy (FE-SEM)

The morphology of the core-shell and the hollow core-shell particle was observed by FE-SEM (JSM-6500, JEOL). Diluted binder solution was dried on the aluminium foil.

2.3.2. High resolution - Transmission electron microscopy (HR-TEM)

The morphology of the core-shell and the hollow core-shell particle was investigated by HR-TEM (H-8100, Hitachi). Diluted binder solution was dropped on the copper grid for HR-TEM and dried. Dried polymer film on the copper grid should be transparent enough so that the light can pass through the sample.

2.3.3. Fourier transform - Infrared (FT-IR)

An infrared spectrum represents a fingerprint of a sample with absorption peaks which correspond to the frequencies of vibrations between the bonds of the atoms making up the material. Because each different material has a unique combination of atoms, no two compounds produce the exact same infrared spectrum. Therefore, infrared spectroscopy can result in a positive identification (qualitative analysis) of every different kind of material.

Alkalization process was analyzed by fourier transform infrared (FT-IR, Nicolet IR 200, Thermo Scientific) searching ionized carboxyl salt. The FT-IR was conducted by applying ATR iD7.

2.3.4. Differential scanning calorimetry (DSC)

DSC (Q20, TA Instruments) with a nitrogen atmosphere and 10 °C/min heating/cooling was used to check the glass transition temperature (T_g) of the polymers. The observation range is from -30 °C to 200 °C. The binder sample was put in an aluminium pan (Tzero Hermetic aluminum pan) and sealed

2.3.5. Thermogravimetric analysis (TGA)

TGA (Q50, TA instruments) was conducted to investigate the thermal stability of polymers with a nitrogen atmosphere and 10 °C/min heating, using TA Instruments Q50. The synthesized polymers were dried and heated up to 900 °C. A platinum pan was used to hold the sample

2.3.6. Particle size analysis (PSA)

The particle size and size distribution of the polymer binder solution was measured by PSA (S3000, Microtrac) based on a laser diffraction light scattering technique. Little amount of binder sample was dropped into an aqueous medium and a tri-layer system analyzes the signals to give the results of size and size distribution.

2.3.7. Dispersion stability

Dispersion stability of binder solution was measured by Turbiscan (Ageing characterization :Turbiscan LAB, Formulaction). For 24 hours, the machine injects light to the solution changing height and analyzes back scattering of light. Because back scattering of light is affected by particles in the solution. This machine can measure the sedimentation, clarification and aggregation etc..

2.3.8. Ionic conductivity

The ionic conductivities of binder solutions were measured by conductivity meter (S230-K, Mettler-Toledo) after calibration.

2.3.9. Adhesive force

Mechanical adhesive force of coated slurry on the current collector was measured by 180° peel test using a texture analyzer (TA-PLUS, Lloyd Instrument Ltd.). To endure the strain from a volume expansion that occur by galvanostatic charge and discharge, adhesion strength is the most important property. Using slitted electrode which width is 2 cm, none-coated face was attached to the double-side tape. And scotch magic tape of 3M was attached to coated face of the electrode. To make whole surface attached uniformly, automatic roll press was used. Finally, top side of the machine pulled the scotch magic tape, the adhesive force was measured and recorded as the scotch magic tape was peeled off from the surface of coated face of electrode.

2.3.10. Contact angle

First, the polymer film was prepared. Binder sample was mixed with CMC and little amount of conductive material, Super-P. And mixed slurry was coated on the copper current collector and dried in a convection oven at 60°C. The binder film was pressed and specimens were prepared in 2 cm × 2 cm size. Specimens were attached on a glass substrate by a double-sided tape. An optical tensiometer (Theta Lite, Biolin Scientific) measured the contact angle of the binder film for 1 min starting from exposing to a drop of electrolyte. Both of electrolytes of EDLC and LIB were tested.

2.3.11. Electrolyte uptake

Specimens were prepared as same way in contact angle test. They were soaked in electrolyte and weighed as time goes by. Both of electrolytes of EDLC and LIB were tested.

2.4. Electrochemical characteristics

2.4.1. Galvanostatic charge and discharge test

Cycle performance and rate capability are typical electrochemical properties. In the test of LTO anode of LIB for the cycle performance, Cells were cycled at the rate of 0.1 C for the first 2 cycles and at the rate of 1 C for the subsequent 98 cycles in a range of 1 V and 2.6 V. For the test of rate capability, they were cycled at the rate of 0.1 C for the first 2 cycles and 0.2 C, 0.5 C, 1 C, 2 C, 5 C, 10 C for 6 cycles at each current, finally 0.1 C again for 2 cycles. Otherwise, in the test of EDLC for the cycle performance, capacity was measured first at the rate of 10 mA/cm² from 0.1 V to 2.7 V at which constant voltage mode was done for 30 min for the first 5 cycles. From the result, 10 mA/F current was calculated and applied from 0.1 V and 2.7 V, no constant voltage mode, for 500 cycles. In the test of rate capability of EDLC, 1, 5, 10, 50 and finally 1 mA/cm² of current were applied for 8 cycles at each rate. all of above tests were conducted by battery cycler (PNE solution Co., Korea).

2.4.2. Cyclic voltammetry (CV)

CV (VSP, BioLogic Science Instruments) of electrode was measured at the various scan rate to investigate the redox reaction in a cell and operating voltage. For the LTO anode of LIB, scan rates were 0.1, 0.5, 1, 2, 5, 10, 20 mV/s and the voltage range was from 1 V to 2.6 V. On the other hand, for the EDLC, scan rates were 5, 20, 50, 100 mV/s and the voltage range was from 0.1 V to 2.7 V. Diffusion coefficient of ions in the cell was calculated by Randle-sevcik equation.

2.4.3. electrochemical impedance spectroscopy (EIS)

EIS (VSP, BioLogic Science Instruments) was measured, for the LIB, at the frequency range from 1 mHz to 1 MHz and at the operating voltage, 1.55 V, after CV test. For the EDLC, EIS was measured at the frequency range from 1 mHz to 1 MHz at the voltage of 0.1, 0.5, 1, 2, 2.7 V after CV test. AC voltage amplitude was 5 mV.

3. Results and discussion

3.1. Physical Characteristics

3.1.1. FE-SEM and HR-TEM results

First, from the figure 9, core alkalization was checked. Most of colloidal core particles were dissolved and became a kinds of film. From the figure 10, it is clearly seen that some holes appeared on the shell while the copolymer in the core is dissolved out. Dissolved ionized polymers were crystalized on the hollow core shell particle. Certainly, from the figure 11, while process is being done, several cracks appear on the shell because of leakage of ionized polymer which has –COO- from the neutralization of MMA-BA-MAA and hydroxide anion. As swelling occurred into the particle, the core space expanded and the color changed following the trace of leakage of inner material.

3.1.2. FT-IR results

To investigate alkalization, 4 samples were used. From the figure 12, comparing Core, Alkalized core and Core shell, Hollow core shell, existence of carboxyl group and ionized carboxyl salt (1500 ~ 1600 nm) can be confirmed. While Core and Core shell samples don't have any peak in 1500 ~ 1600 nm, Alkalized core and Hollow core shell samples certainly have peaks in 1500 ~ 1600 nm. It shows that MMA-BA-MAA copolymer decomposed to polymer ion which has –COO-. Polymerization of acrylonitrile and styrene also was confirmed.

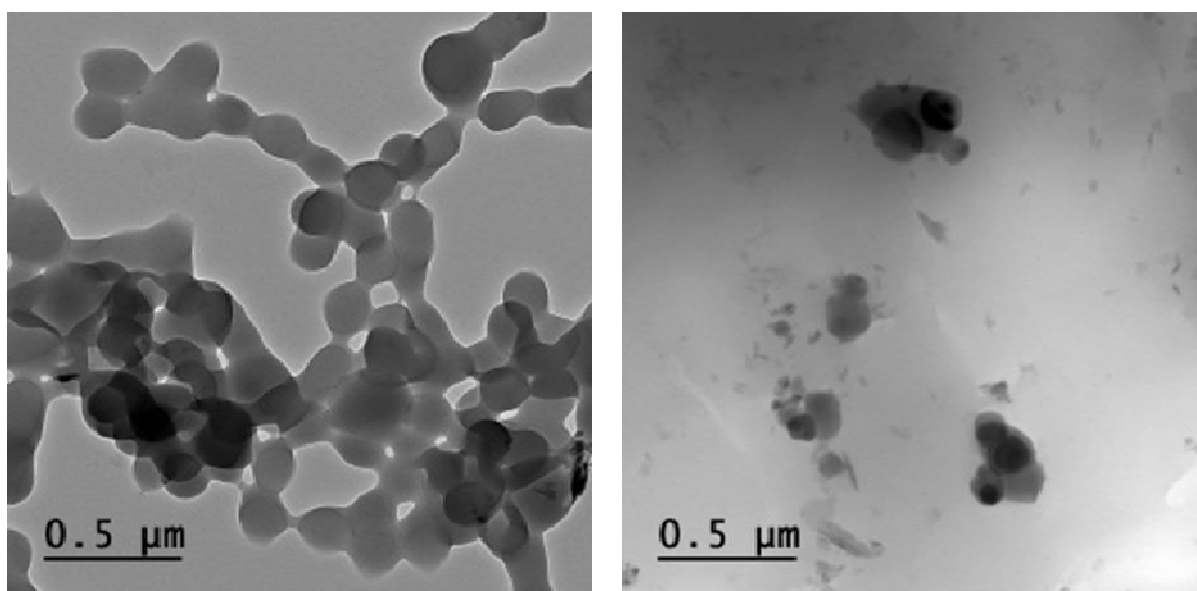


Figure 9.HR-TEM results of Core (left) and Alkalized core (right)

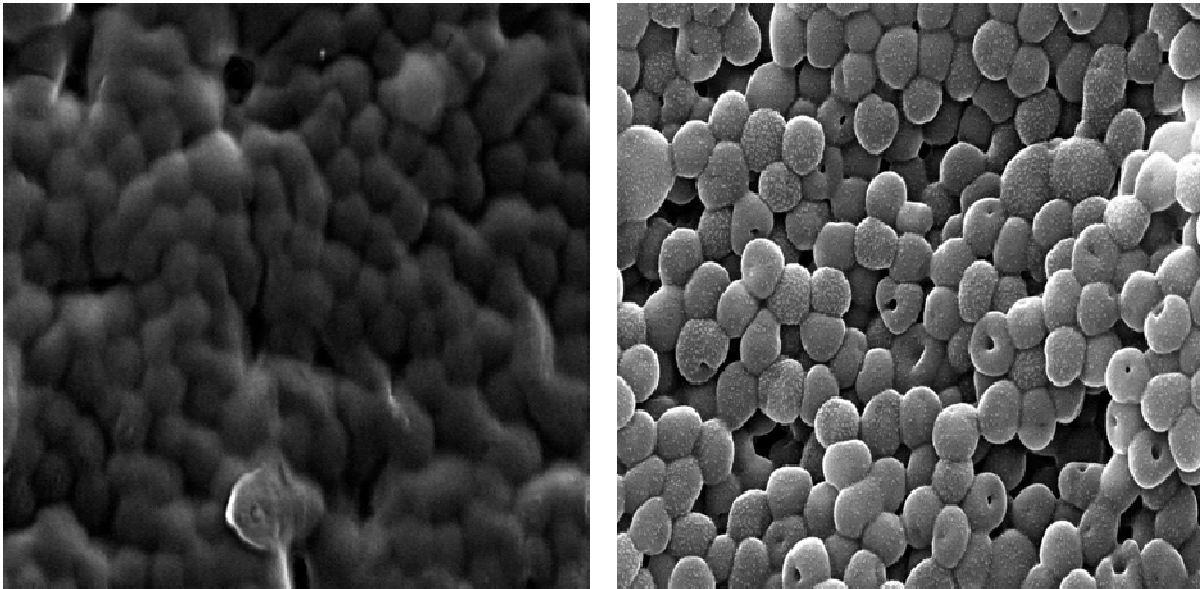


Figure 10.FE-SEM results of Core shell (left) and Hollow core shell (right)

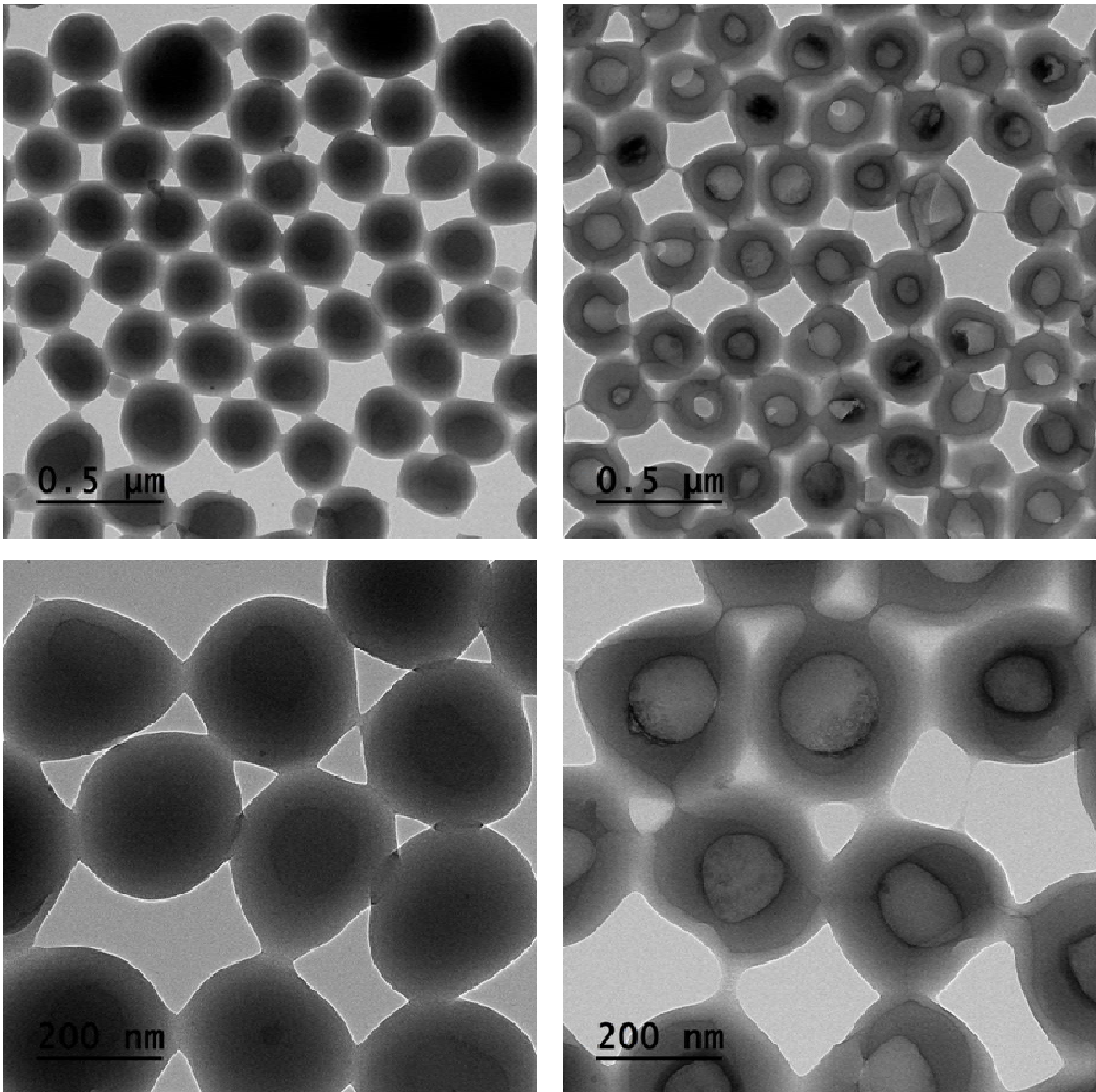


Figure 11.HR-TEM results of Core shell (left) and Hollow core shell (right)

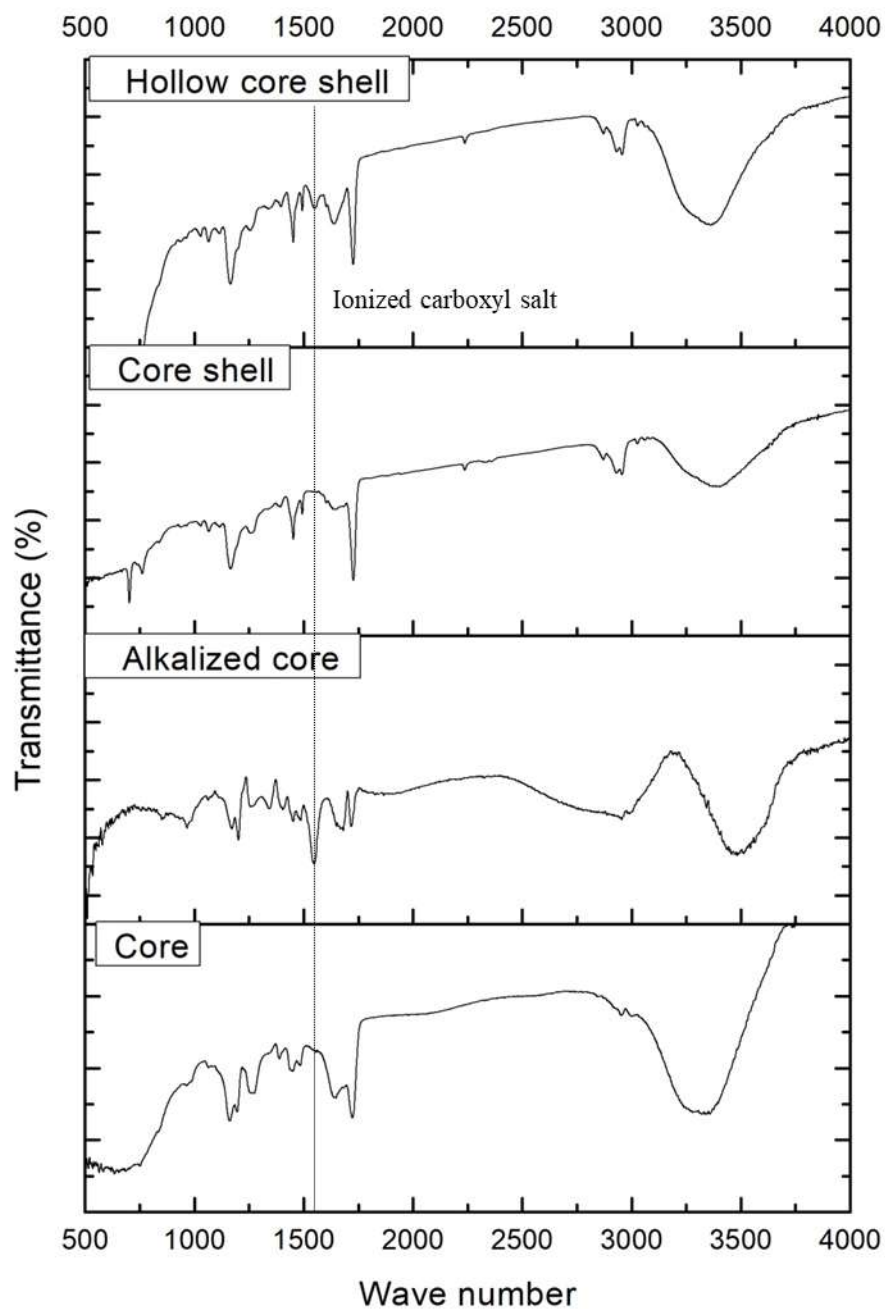


Figure 12. FT-IR results of Core, Alkalized core, Core shell and Hollow core shell

3.1.3. DSC, TGA, PSA results

First, from DSC results, glass transition temperature of MMA-BA-MAA core copolymer is around 170 °C. And in the DSC result of alkalized core, there is a peak at 175 °C. It means that crystal of ionized core polymer decomposed at that temperature. This is confirmed again in TGA result of alkalized core. Many side peaks appeared in TGA result of alkalized core because of strong base, NaOH. The glass transition temperature of shell polymer is around 400°C. Other small peaks in TGA results of Core shell and Hollow core shell samples may well be side products of non-reacted monomers including all of core and shell stage monomers. From PSA results, Size distribution is quite good. After alkalization, average of particle size increased. It may happen because core copolymer decomposed and tried to go out from the particle, then shell would be forced to expand outside and finally holes came up by pressure. Also solvent got inside the core and wet inside, which is called swelling, then particle size can be increased. On the other hand, little amount of aggregation happened so some particles larger than 1.5 µm were formed. Because NaOH changed pH strongly and stability of solution became bad.

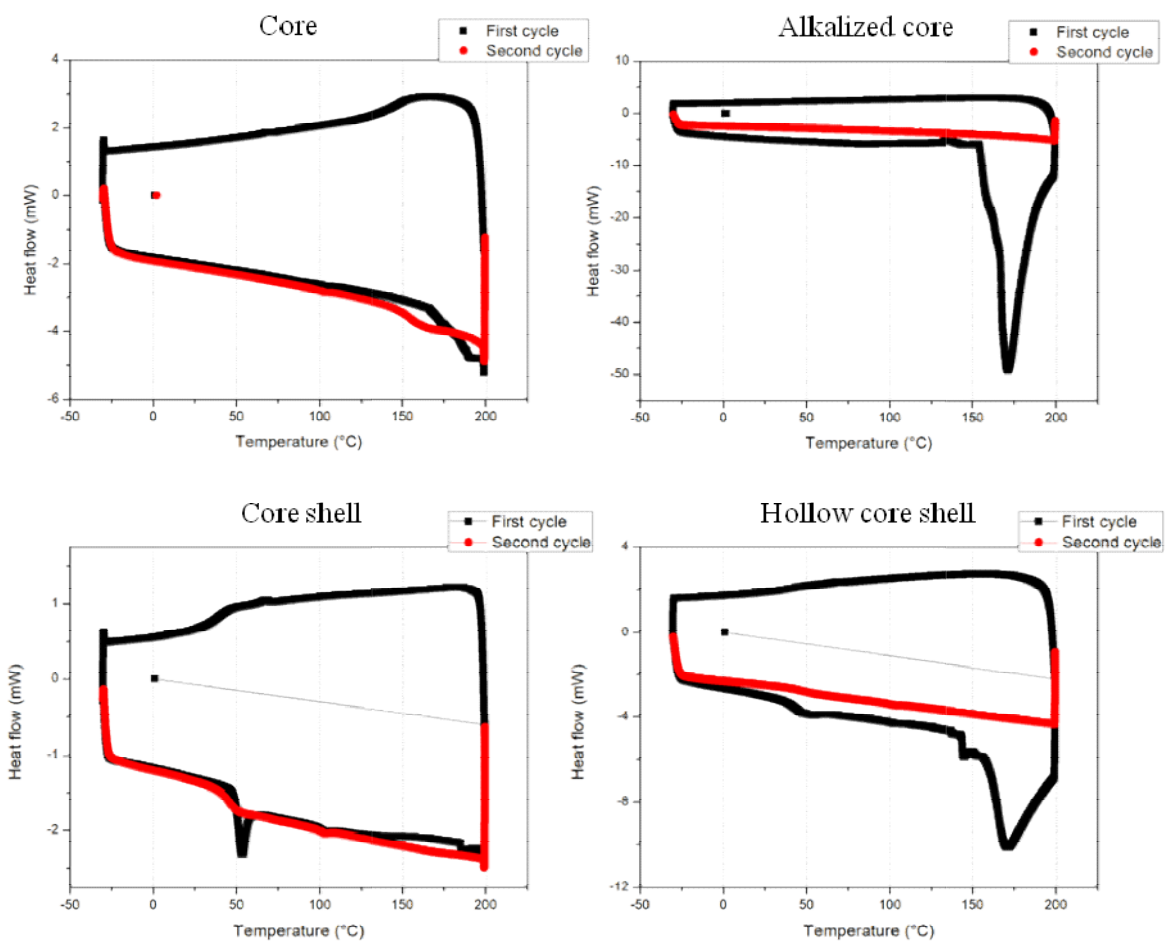


Figure 13. DSC results of Core, Alkalized core, Core shell and Hollow core shell

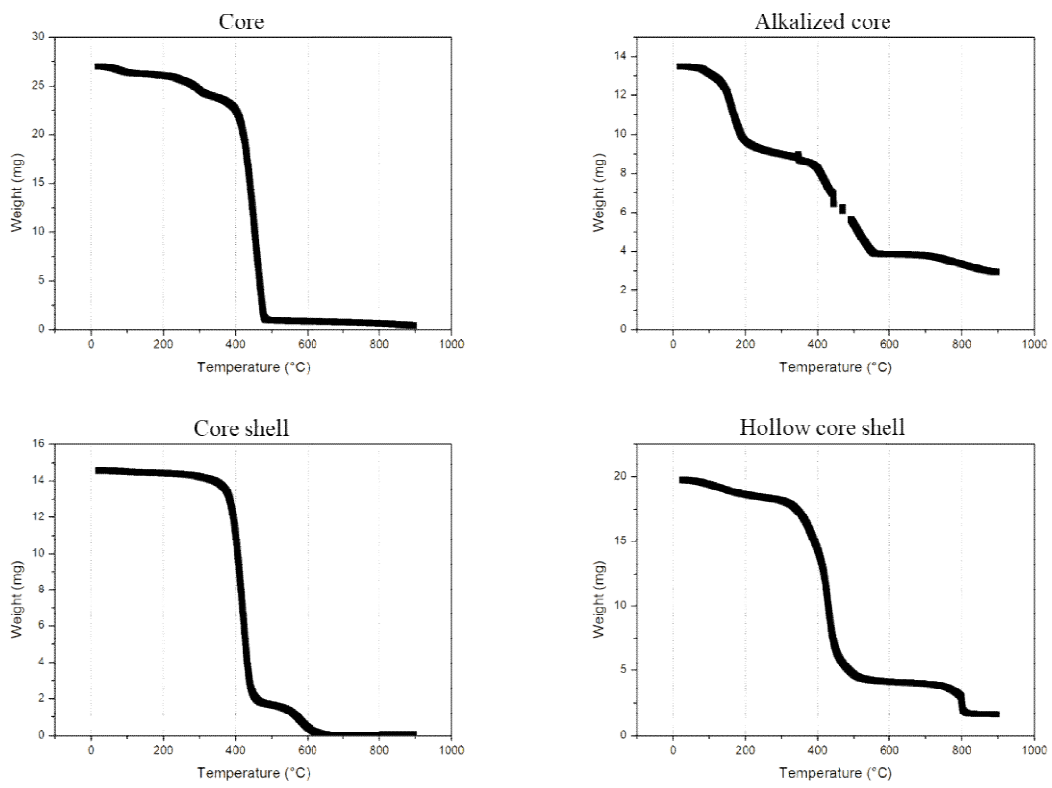


Figure 14. TGA results of Core, Alkalized core, Core shell and Hollow core shell

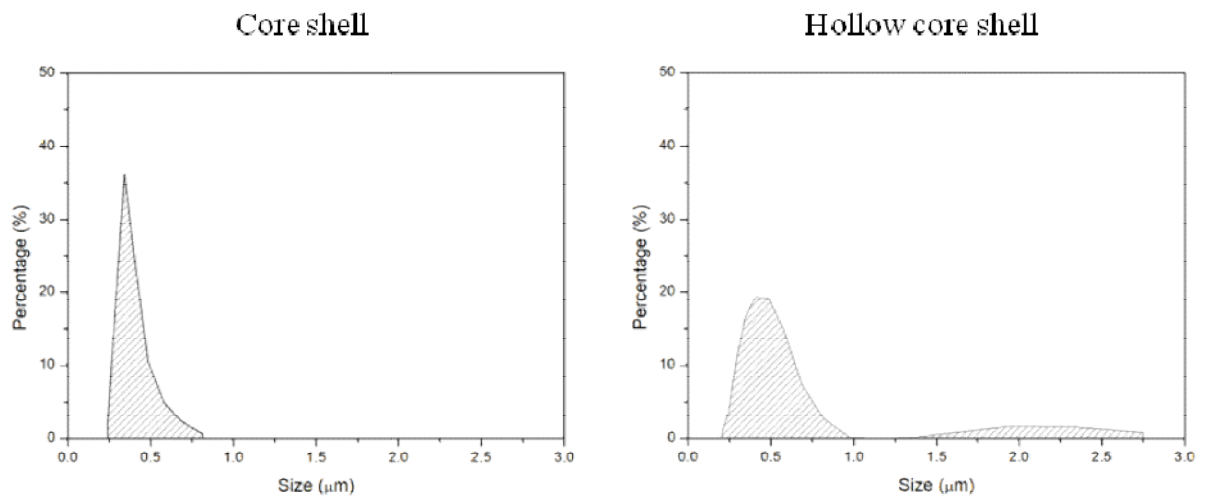


Figure 15.PSA results of Core shell and Hollow core shell

3.1.4. Dispersion stability results

First of all, from the figure 17 and figure 18, change of turbiscan stability index (TSI) is larger in Hollow core shell sample. Even though SBR 400B is the commercial final product from ZEON, global stability is not that different with Core shell sample. Therefore, Core shell sample could be more stable after stabilization such as adding dispersion agent or removing non-reacted monomers. From the back scattering data of SBR 400B, Delta back scattering goes up to 3.5 in the beginning, which means that sedimentation happened on the bottom side of solution. However, Delta back scattering goes down to -1 in the end, which means that little amount of aggregation occurred. On the other hand, Delta back scattering goes down to -2 in the beginning, which means that clarification occurred following sedimentation of bottom side. But Delta back scattering goes up to 5 again in the end, which means that suspended solids appeared. From the back scattering data of Core shell sample, sedimentation happened at the bottom of solution. As expected, because the particle size is not small enough, the top of the solution was clarified a lot as particles sank down. Therefore Delta back scattering goes down to -25. On the other hand, in the Hollow core shell sample, Delta back scattering is negative. Also in the middle of solution, the width of graph line is thicker. This means aggregation. Because the viscosity of solution is high and the particles are adhesive, sediments get close enough, finally, the machine define as a big particle of aggregation. If this happens strongly, sediments cannot be dispersed again. Even though, there is big difference of delta back scattering of top side of each solution. Amounts of sedimentation and aggregation are similar. Also in real, there is no problem to re-disperse and even no flocculation.

Stability - SBR 400B

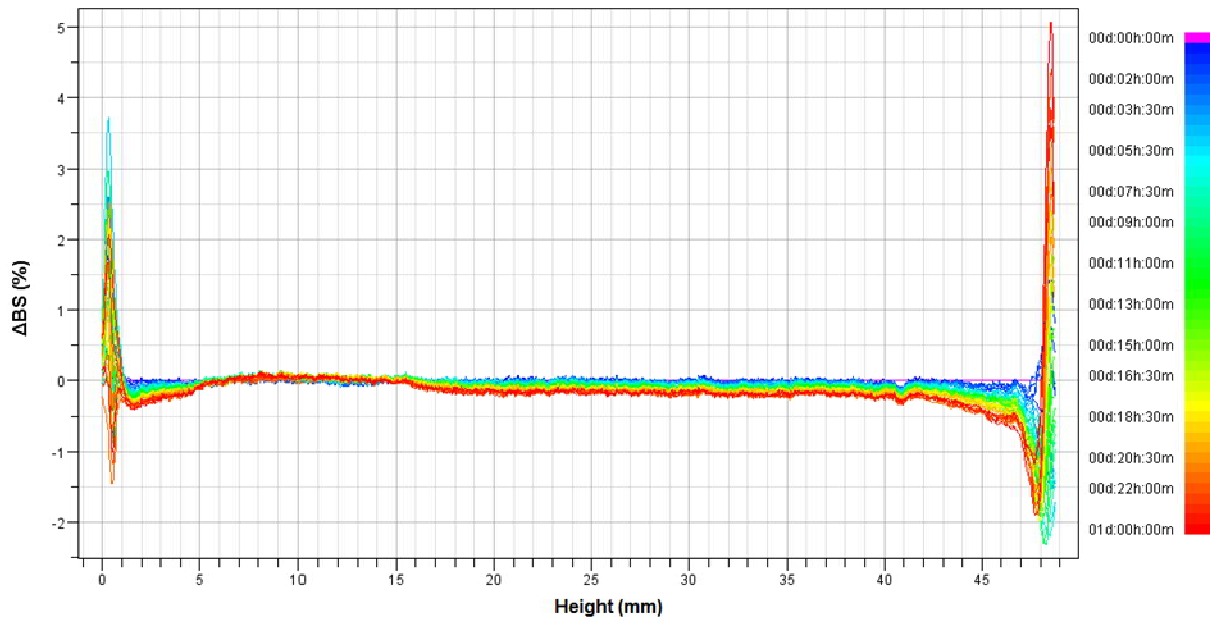
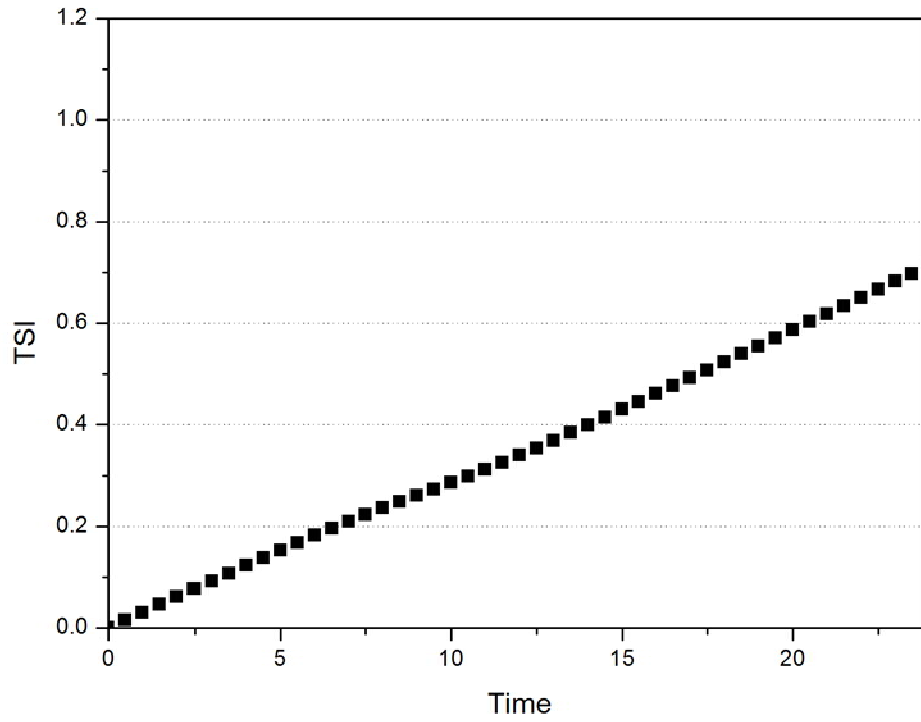


Figure 16. Turbiscan results of SBR 400B

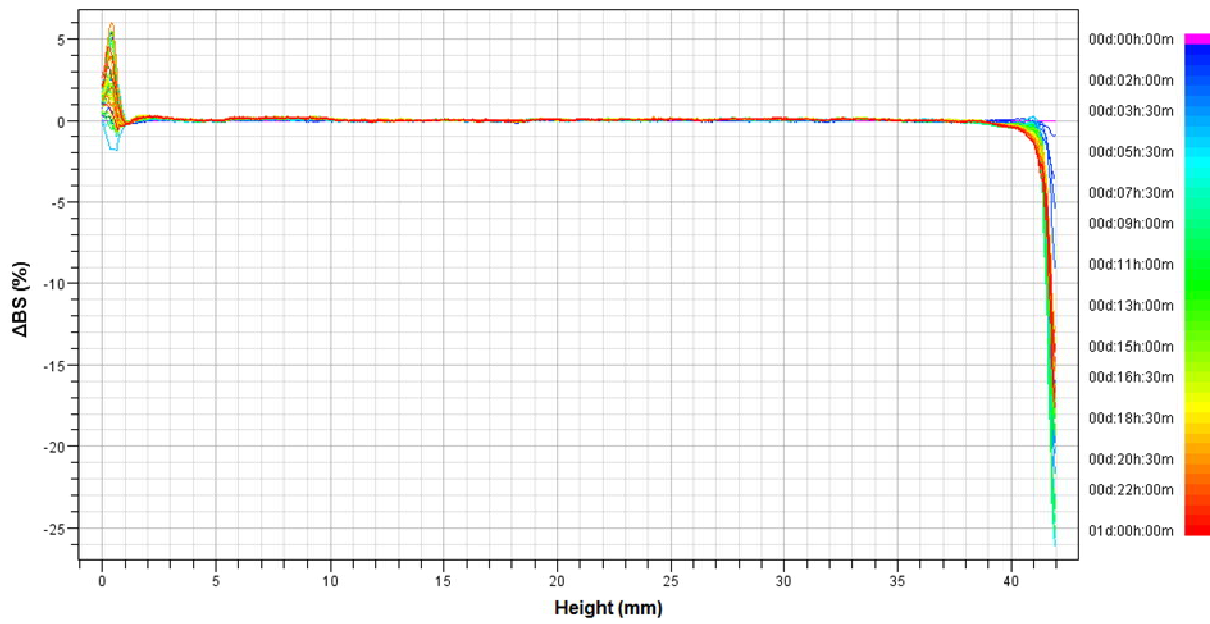
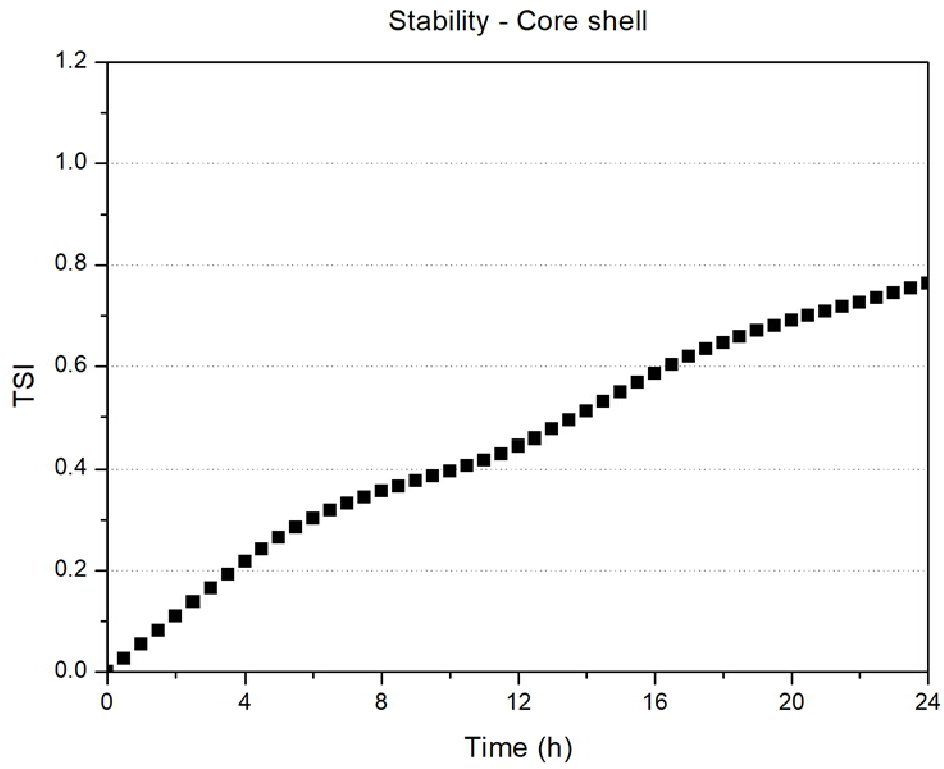


Figure 17. Turbiscan results of Core shell

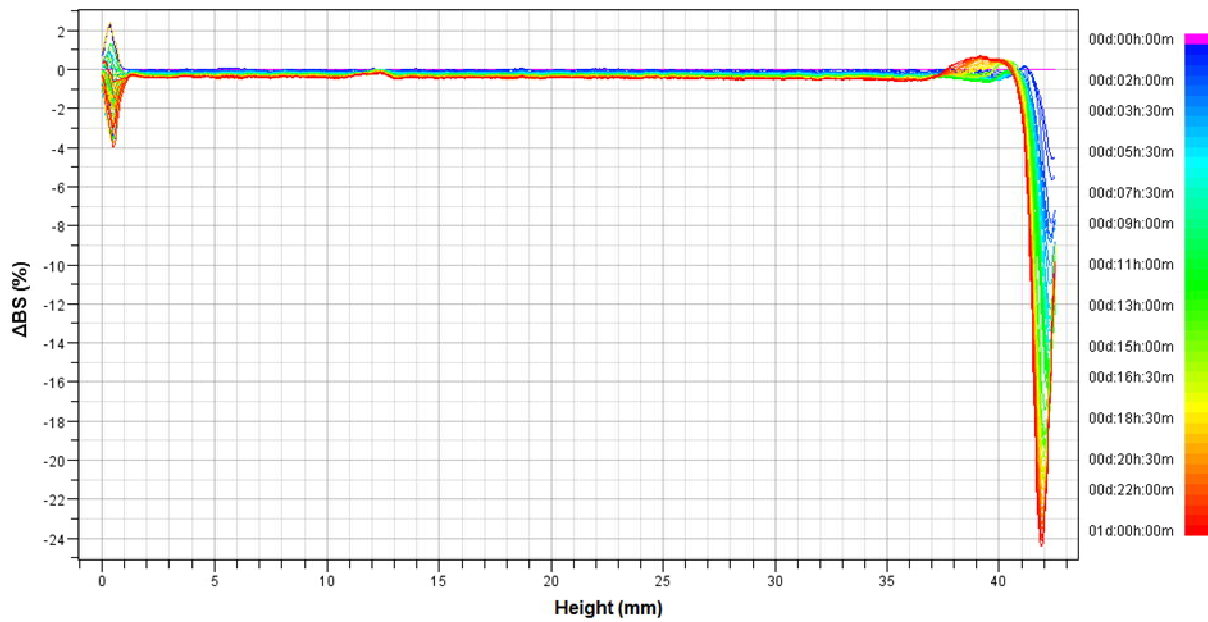
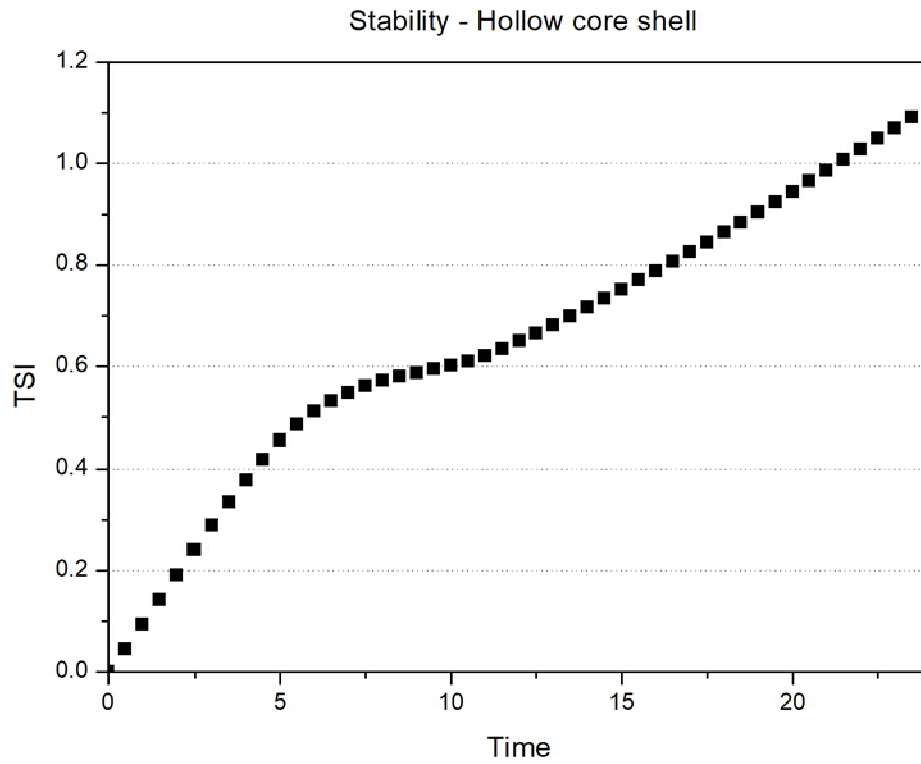


Figure 18. Turbiscan results of Hollow core shell

3.1.5. Ionic conductivity results

From the figure 18, even though acrylonitrile was used as shell monomer to make ionic conductivity higher, ionic conductivity of Core shell sample is not that different with SBR sample. But It is definite that ionized MMA-BA-MAA core polymer increases the ionic conductivity a lot. Although that ion increases the viscosity also which can make the ionic conductivity low, charge of polymer ions in the solution helps other ions easily to migrate.

3.1.6. Contact angle results

Contact angle test was conducted and investigated at 0 s start point and 60 s end point. By investigating contact angle, affinity of binder with electrolyte can be observed. Affinities of each binder samples with EDLC electrolyte are quite similar. However, unlike an expectation, affinity of Hollow core shell (HCS) sample with LIB electrolyte is not that better whereas Core shell (CS) sample's affinity with LIB electrolyte is good. This means shell stage which is St-BA-AN copolymer is friendly enough with electrolyte following reference, though, crystal of core stage which is MMA-BA-MAA copolymer is not friendly with electrolyte.

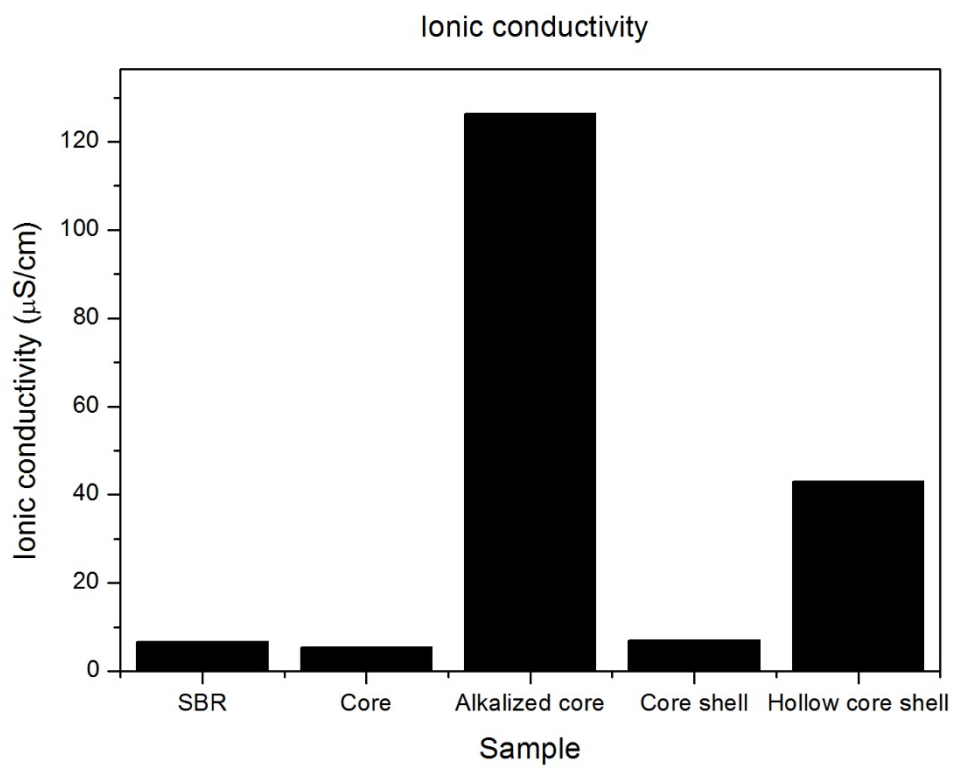
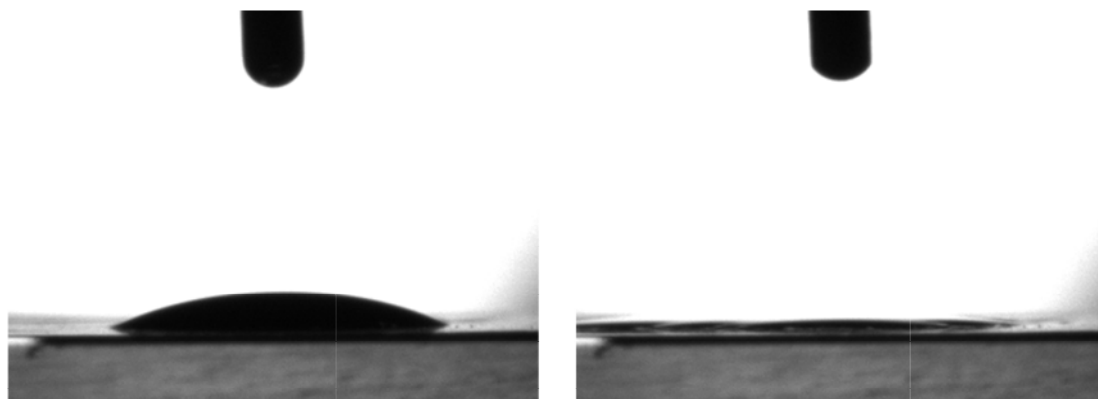
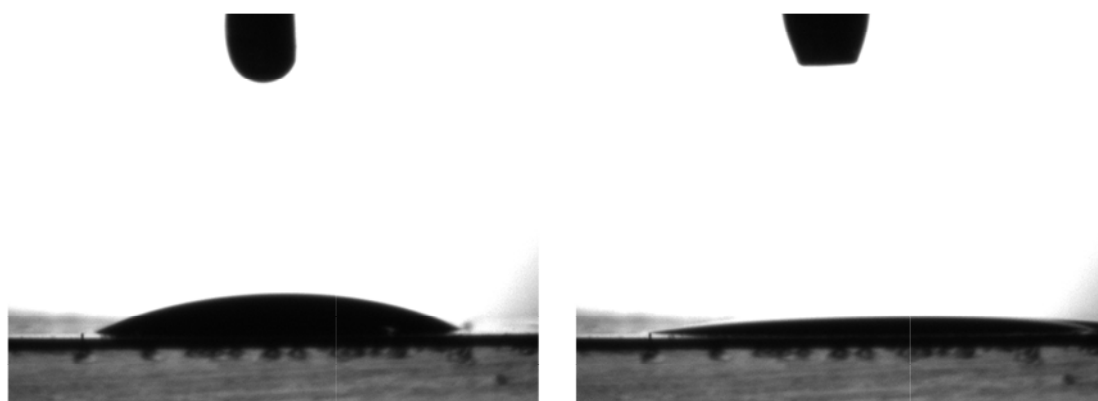


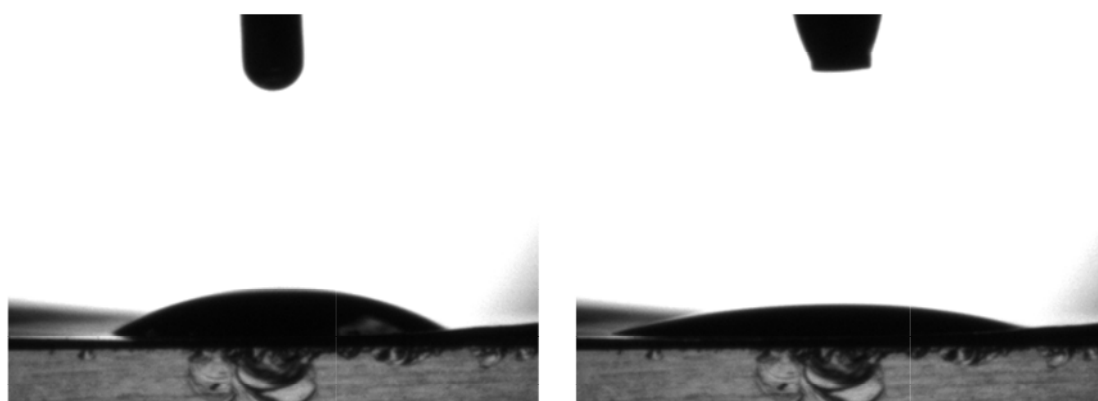
Figure 19. Ionic conductivity results of SBR, Core, Alkalized core, Core shell, Hollow core shell



SBR-LIB Start and End



CS-LIB Start and End



HCS-LIB Start and End

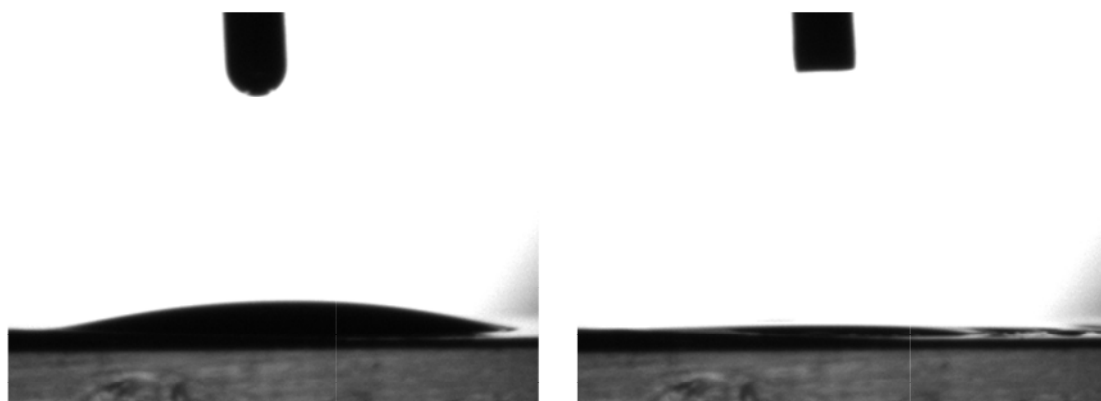
Figure 20. Pictures of contact angle between each of binder films and LIB electrolyte.



SBR-Capa Start and End



CS-Capa Start and End



HCS-Capa Start and End

Figure 21. Pictures of contact angle between each of binder films and EDLC electrolyte.

Binder-Electrolyte	Start (°)	End (°)
SBR-LIB	26.36	4.49
CS-LIB	25.01	5.92
HCS-LIB	30.21	15.49
SBR-Capa	15.6	3.48
CS-Capa	15.42	0
HCS-Capa	13.2	2.97

Table2.Contact angle results of SBR, CS and HCS with LIB and EDLC electrolytes

3.1.7. Adhesive force results

From the adhesive test of binder films, adhesive forces of binders were defined absolutely except other parameters. Certainly, SBR binder is the most adhesive binder. HCS binder also showed similar adhesive force with SBR binder which is reference. However CS binder film showed noticeably low adhesive force. This result might be from the structure of the particle and viscosity. First, CS binder film is more fragile than HCS binder film. Because the hollow structure made the particles more flexible and elastic. Also, normally the higher viscosity, the stronger adhesive force.

Adhesive test

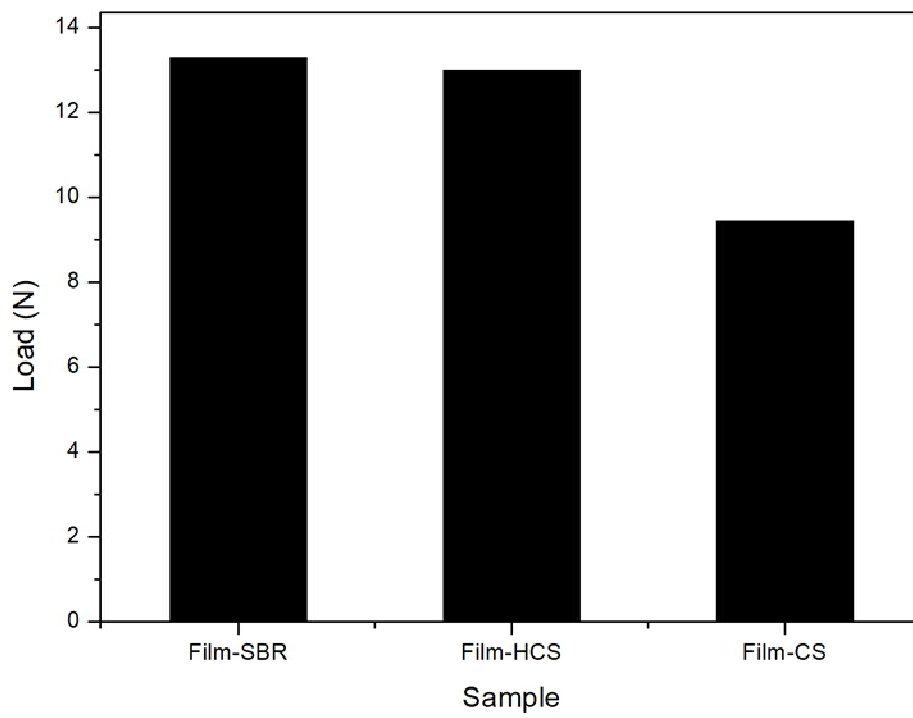
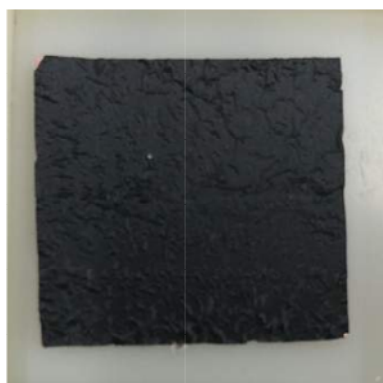


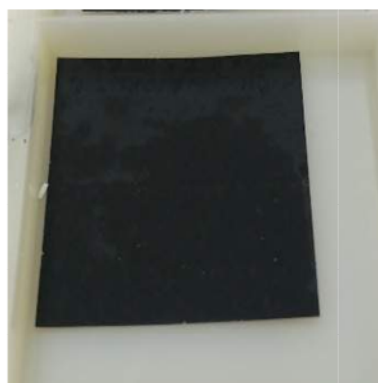
Figure 22.Adhesive force results of binder films of SBR, CS and HCS binders

3.1.8. Electrolyte uptake results

From the electrolyte uptake result, It is investigated how much electrolyte the electrode can keep inside. And especially as electrode is stored and soaked in electrolyte for a long time, reaction or dissolution of binder can be investigated. Also collapse of coated structure can be happened. In figure 23, as CS and HCS binder film absorbed the LIB electrolyte, It looks that binder film become wet and diminished. At the contact angle test, it was checked that core copolymer is not friendly with LIB electrolyte. However, it seems that core copolymer contract by absorbing electrolyte as time goes by. As a result, electrode got rolled and detached from the current collector. Electrolyte uptake of SBR-LIB is 3.4 mg. And electrolyte uptake of CS-LIB is 10.8 mg. However electrolyte uptake of HCS-LIB is -3 mg. Core copolymer may absorb a lot of electrolyte. Whereas crystallized core ionized polymer can not absorb lots of electrolyte. And even after being dried, electrolyte was absorbed to the core inside the particle. Therefore, electrolyte wouldn't removed easily. In case of electrolyte uptake result with EDLC electrolyte, there are no big differences between binder samples.



SBR-LIB



SBR-EDLC



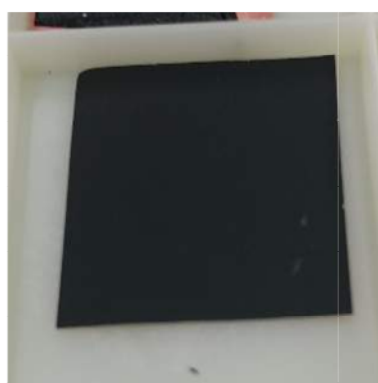
CS-LIB



CS-EDLC



HCS-LIB



HCS-EDLC

Figure 23. Pictures of binder films soaked in electrolytes for 144 hours

Binder-Electrolyte	Start	Dried after 144h
SBR-LIB	64	67.4
CS-LIB	68.7	79.5
HCS-LIB	65.7	65.4
SBR-Capa	68.9	70.2
CS-Capa	67.2	70.2
HCS-Capa	66.9	67.8

Table 3.Weights (mg) of binder films at the beginning and fully dried after 144 hours

3.2. Electrochemical characteristics

3.2.1. Cycle and rate capability results of LTO anode

There is not that big difference of capacity of each samples. However durability of CS is the best. In the cycle test, the amount of capacity decrease of CS is the lowest. Likewise in the rate capability test, CS sample showed the highest performance in high rate. This might mean that even though CS binder showed lowest adhesive force, it is quite enough to endure high current. Also MMA-BA-MAA copolymer in the core space of CS binder is more helpful to conductivity than hollow core. However HCS sample showed lower performance than SBR reference binder.

3.2.2. CV results and calculation of diffusion coefficient of LTO anode

First, from the CV results, CS binder showed lowest conductivity in the cell. However CS binder showed current at around 2.6 V. This means that decomposition of polymer binder or shift of operating voltage. In the cycle and rate capability test, durability of CS binder was checked. Therefore it is not the decomposition of binder. Overall none of binder samples has decomposition. By the Randles-Sevcik equation, diffusion coefficient was calculated. By the slope of the peak current vs. the square root of the scan rate, chemical diffusion coefficient of lithium-ion (DLi) in LTO electrodes can be calculated according to the Randles-Sevcik equation

$$i_p = 268,600 n^{3/2} C_{Li} A D_{Li}^{1/2} v^{1/2} \text{ (at } 25^\circ\text{C)}$$

where i_p is the peak current, n is the number of electrons pertaining to the redox reaction (for Li^+ , it is 1), C_{Li} is the initial concentration of lithium ion, A is the surface area of the electrode, D_{Li} is the diffusion coefficient and v is scan rate [17]. From this equation, the diffusion coefficients of SBR binder electrode, CS binder electrode and HCS binder electrode can be computed. As a result, diffusion coefficients of CS binder sample in both case of charge and discharge are the lowest. However CS sample showed low peak current but some other peaks near 2.6 V. So it showed lowest diffusion coefficient but also highest cell performance.

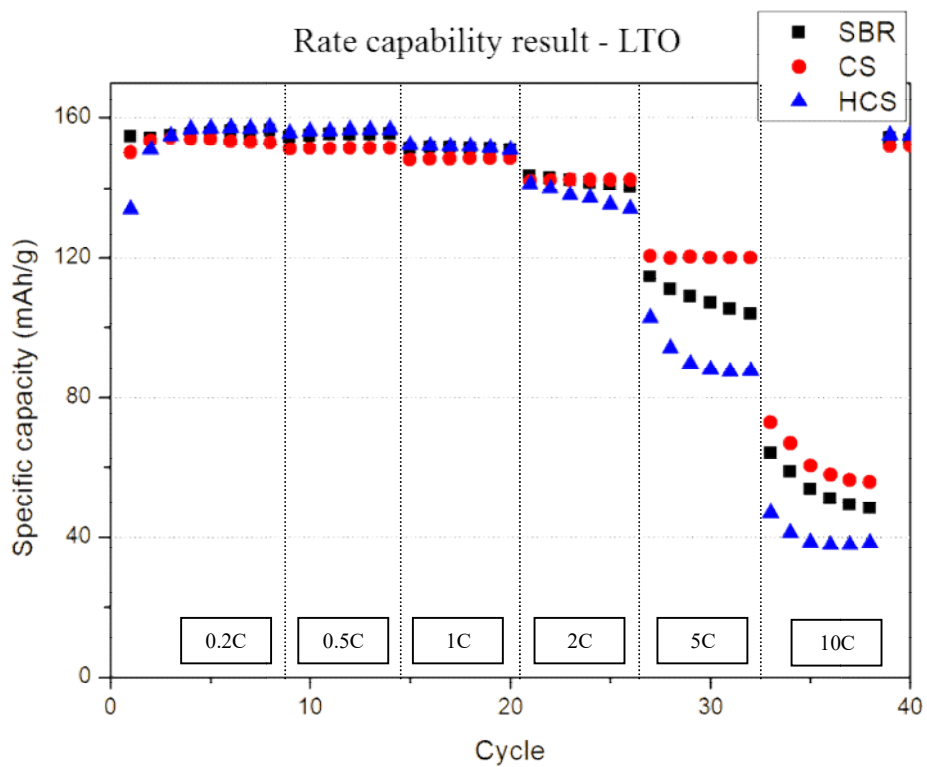
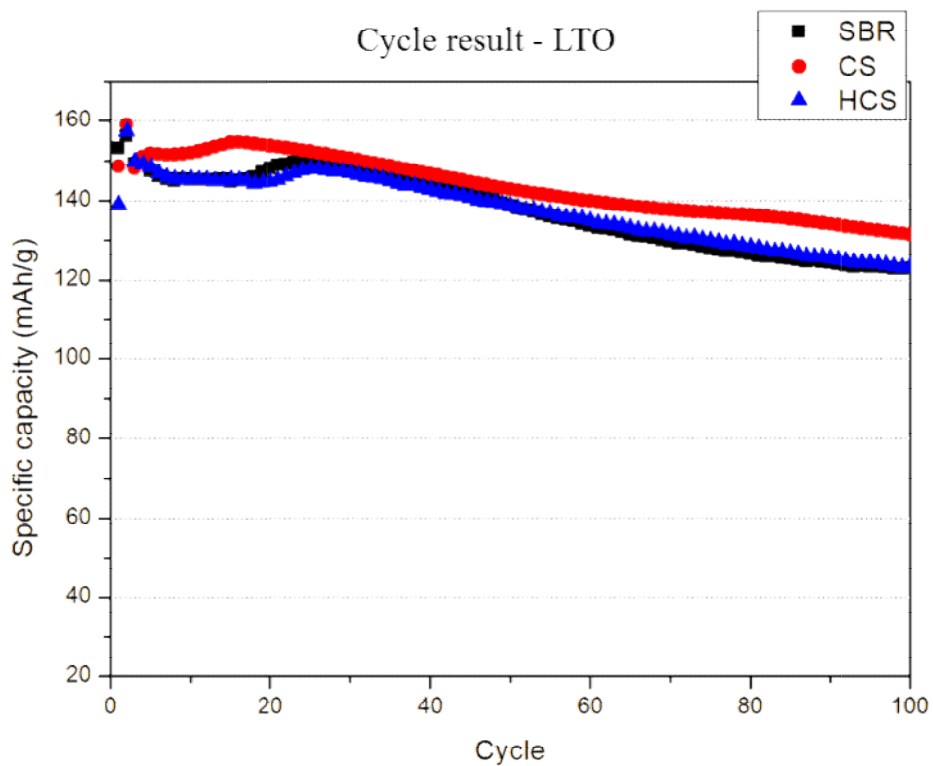


Figure 24. Cycle and rate capability data of LTO cells comparing SBR, CS and HCS binders

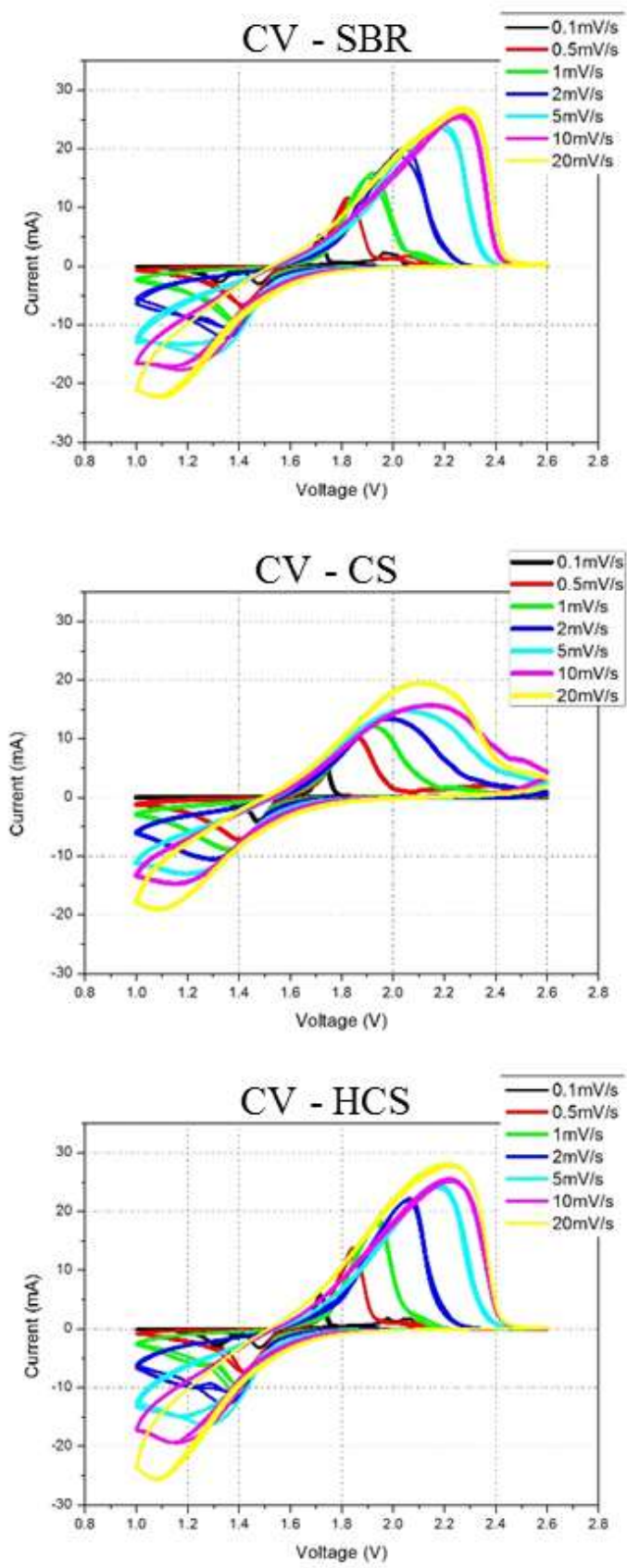


Figure 25. CV data of LTO cells comparing SBR, CS and HCS binders

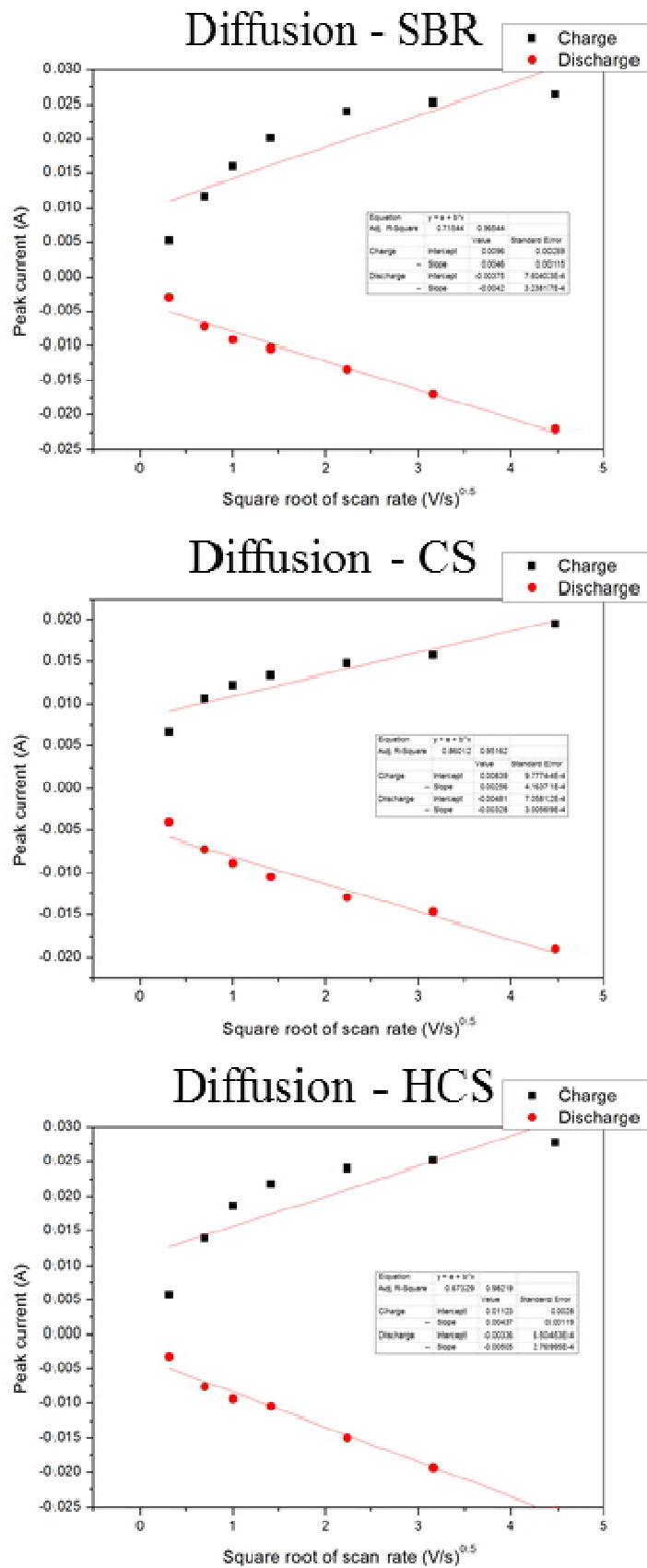


Figure 26. Computation of slope of peak currents vs. square root of voltage scan rate of LTO cells comparing SBR, CS and HCS binders from Randle-sevcik equation

	Diffusion coefficient (Charge)	Diffusion coefficient (Discharge)
LTO-SBR	1.2383E-22	1.03231E-22
LTO-CS	3.83522E-23	6.29591E-23
LTO-HCS	1.11757E-22	1.49243E-22

Table4.Diffusion coefficient of LTO cells of both of SBR, CS and HCS samples

3.2.3. EIS results of LTO anode

From the EIS result, resistance of bulk solution (R_s), charge transfer resistance (R_{ct}), resistance to the bulk of active material which is also called Warburg impedance (R_{diff}) can be observed. All of these resistances should be observed at operating voltage at which redox reaction is happening.

$$Z_{re} = R_s + R_{ct} + R_{diff}$$

First point of first semicircle is R_s . And Diameter of first semicircle is R_{ct} . Finally R_{diff} is the length of the 45° straight line in the end of graph before slope suddenly changes. First, normally LTO cell doesn't have Solid electrolyte interphase (SEI). However CS and HCS sample showed second semicircle which means some layer. Definitely, resistance in the bulk electrolyte of CS sample is the lowest. MMA-BA-MAA may help conductivity in the bulk electrolyte. Also hollow structure has lower resistance than SBR binder. However charge transfer resistance of CS is pretty high. From second semicircle, it is defined that one layer was produced on the surface of electrode. In the CS cells, it is more difficult than HCS cells that electrons jump between electrolyte and electrode. This may be from the morphology of hollow core shell. Interphase between electrolyte and active materials become larger.

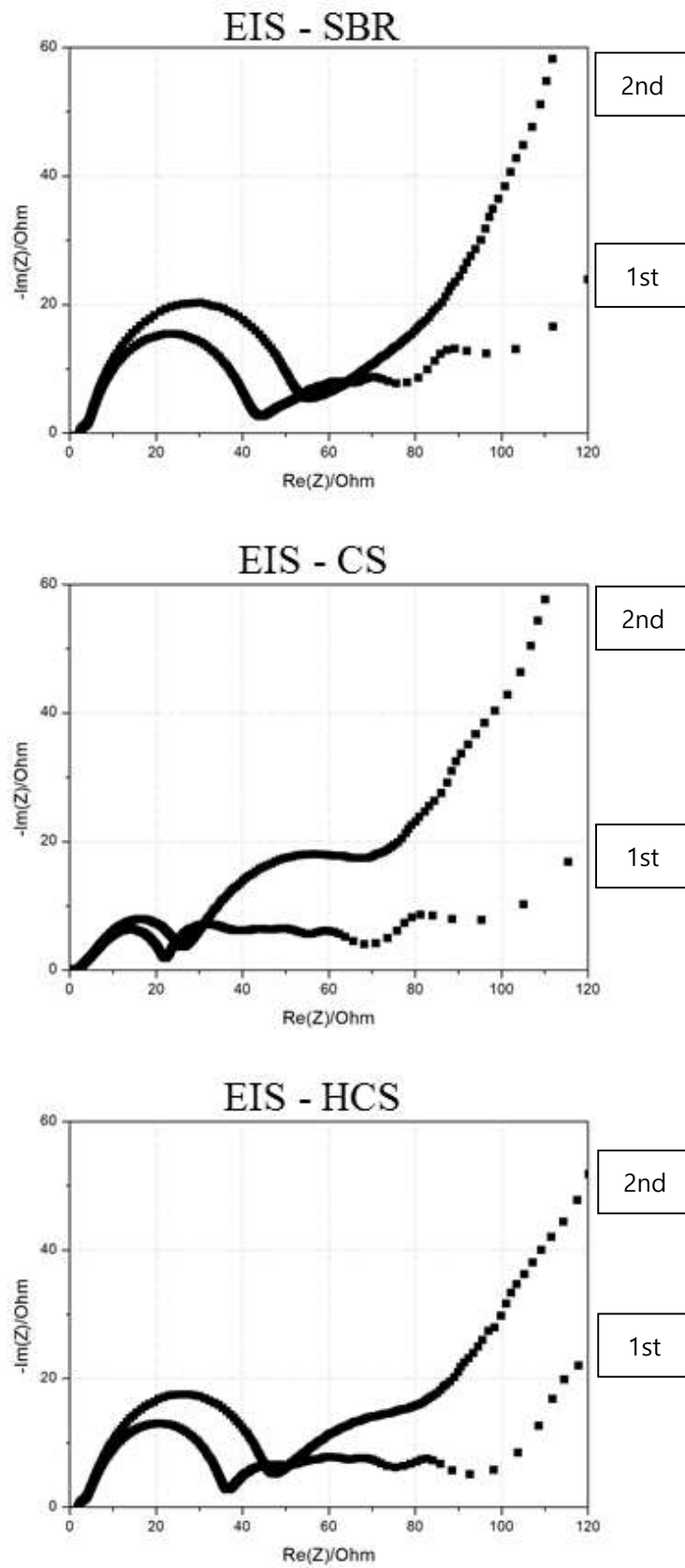


Figure 27. EIS data of LTO cells comparing SBR, CS and HCS binders

3.2.4. Cycle and rate capability results of EDLC

From the cycle test and rate capability test, likewise LTO test, It is defined that CS binder is the best for the cell performances. But at extremely high current, 50 mA/cm², performance of CS and HCS became lower than SBR. In the low current condition, because diffusion is slow, the morphology of binder particle can be almost used. In short, active materials in the deep side of the electrode can be used. But in the high current condition, before ions pass through the deep side of the electrode and make electric double layer, charge or discharge step would be over. Unfortunately, this can define that except the effect of hollow morphology and MMA-BA-MAA core copolymer, particle itself such as shell stage is not more conductive than SBR reference binder. But even though CS and HCS showed worse performance in the highest rate, when they went back to slow rate, they kept its high performance like before. This means adhesive forces of CS, HCS are enough and even at high rate and strong strain, it can endure the extreme condition.

3.2.5. CV results and calculation of diffusion coefficient of EDLC

Also In CV results of EDLC, CS and HCS binder followed SBR reference binder. Likewise SBR reference, CS and HCS binder don't have any side reaction with the EDLC electrolyte in 0.1 V ~ 2.7 V

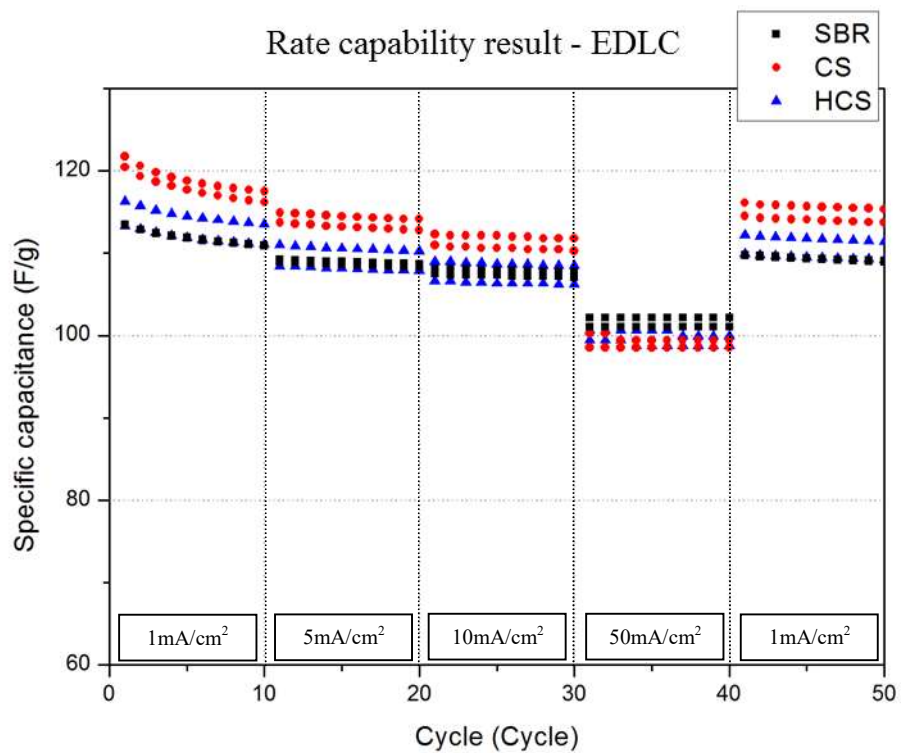
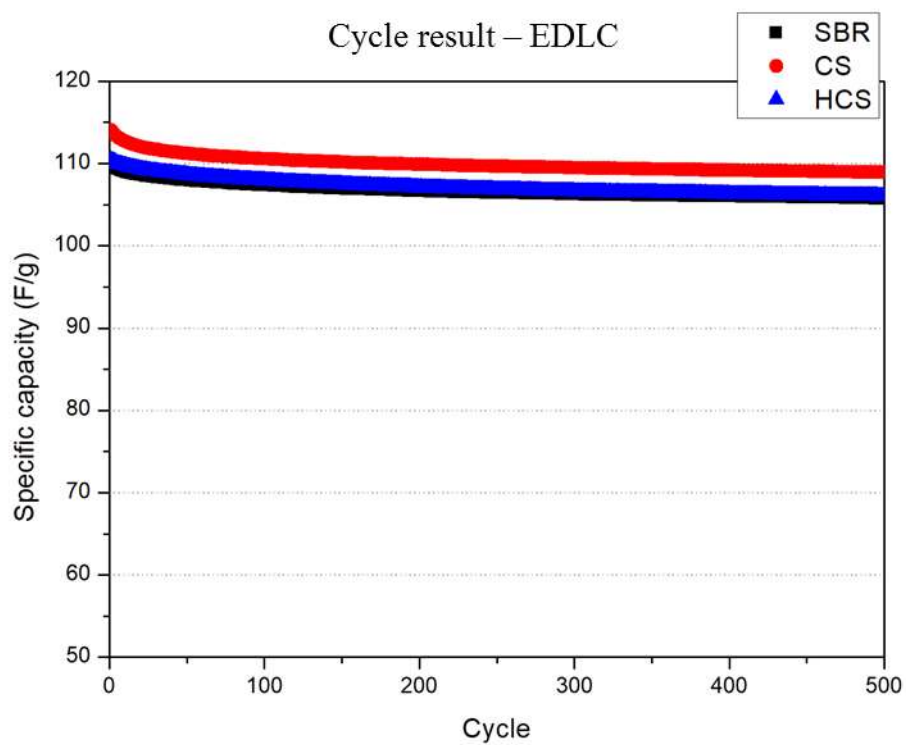


Figure 28. Cycle and rate capability data of EDLC comparing SBR, CS and HCS binders

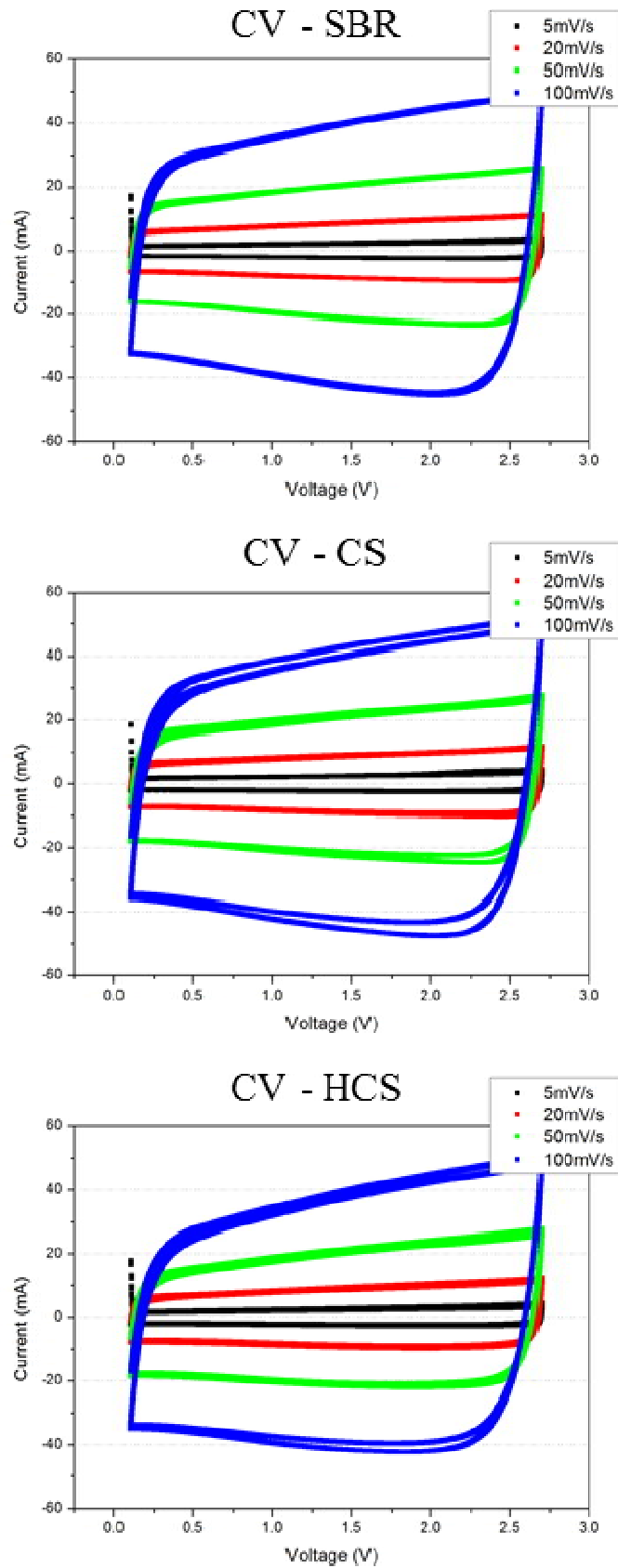


Figure 29. CV data of EDLC comparing SBR, CS and HCS binders

3.2.6. EIS results of EDLC

In EDLC, redox reaction doesn't exist. Therefore, there is no charge transfer resistance. Instead, the semicircle means conductivity of ions from electrolyte to the surface of activated carbon to make charge valance. Overall, CS showed lowest resistance in every voltage scan rate. In case of HCS, as voltage increases, resistance got lower and similar with SBR reference and finally CS.

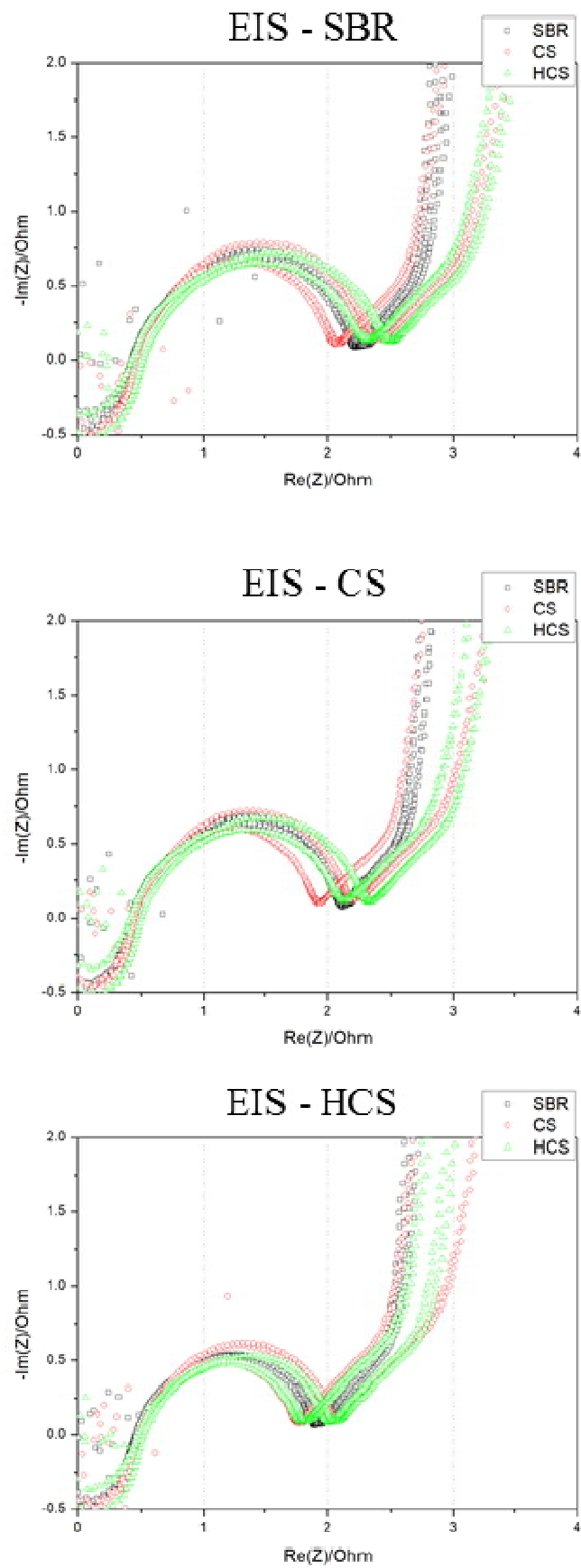


Figure 30. EIS data of EDLC comparing SBR, CS and HCS binders

4. Conclusion

The purpose of this experiment was to make new polymer binder which has better performance to improve electrochemical characteristics of cells. To make hollow polymer with adhesive and ionic conductive materials was succeeded. As a result of comparing SBR reference binder, core shell binder and hollow core shell binder, core shell binder which has MMA-BA-MAA copolymer in the core space showed the best performance in the electrochemical system. It was also checked that hollow structure can help conductivity comparing with the SBR binder. Collectively new polymer binders can replace SBR binder. Furthermore they can be improved by changing ratio of monomers, for example, decreasing ratio of styrene, increasing BA.

5. Reference

- [1] Zaghbi, K., Mauger, A., Groult, H., Goodenough, J., Julien, C., 2013. *Materials* 6, 1028–1049.
- [2] Oh, J., Jin, D., Kim, K., Song, D., Lee, Y.M., Ryou, M.-H., 2017. *ACS Omega* 2, 8438–8444.
- [3] Nitta, N., Wu, F., Lee, J.T., Yushin, G., 2015. *Materials Today* 18, 252–264.
- [4] Liu, C., Neale, Z.G., Cao, G., 2016. *Materials Today* 19, 109–123.
- [5] Shiraishi, S., 2013. 7.
- [6] Zhang, X., Zhang, H., Li, C., Wang, K., Sun, X., Ma, Y., 2014. *RSC Adv.* 4, 45862–45884.
- [7] Nordh, T., Younesi, R., Brandell, D., Edström, K., 2015. *Journal of Power Sources* 294, 173–179.
- [8] Nordh, T., DiVA, 2015.
- [9] Yuan, C.-D., Miao, A.-H., Cao, J.-W., Xu, Y.-S., Cao, T.-Y., 2005. *Journal of Applied Polymer Science* 98, 1505–1510.
- [10] Zhang, Q., Yang, Z., Zhan, X., Chen, F., 2009. *Journal of Applied Polymer Science* 113, 207–215.
- [11] Song, C., Zhang, L., Wang, Y., Yan, X., Zhao, D., 2013. *Journal of Materials Science* 48, 8153–8162.
- [12] Y. Liu, Dr. K. V. Edmond, Dr. A. Curran, C. Bryant, Dr. B. Peng, Prof. D. G. A. L. Aarts, Dr. R. P. A. Dullens, *Adv. Mater.* 2016, 28, 8001–8006.
- [13] Solarajan, A.K., Murugadoss, V., Angaiah, S., *Applied Materials Today* 5 (2016) 33–40
- [14] Lee, B.-R., Oh, E.-S., 2013. *The Journal of Physical Chemistry C* 117, 4404–4409.
- [15] Ramli, R.A., 2017. *RSC Advances* 7, 52632–52650.
- [16] Jeong, J.-H., Jung, D., Shin, E.W., Oh, E.-S., 2014. *Journal of Alloys and Compounds* 604, 226–232.
- [17] Neghmouche, N.S., Lanez, T., 2013. *International Letters of Chemistry, Physics and Astronomy* 9, 37–45.